ANALYTICAL PREDICTION OF THE BEARING STRENGTH OF CONNECTIONS WITH LONG BOLTS

Latour M.[*x], Rizzano G.[*], D'Antimo M. [**], Demonceau J.F.[**], Jaspart J.P.[**], Armenante V.[*]

[*]University of Salerno, Department of Civil Engineering, *mlatour@unisa.it , g.rizzano@unisa.it*

[**]University of Liège, ArGenCo Department, *mdantimo@ulg.ac.be jfdemonceau@ulg.ac.be , jean-pierre.jaspart@ulg.ac.be*

Abstract

This work deals with the prediction of the bearing resistance of elementary shear connections constituted by gusset plates and square hollow sections fastened with long bolts. The research is motivated by the lack of specific rules in international codes for this particular configuration. In fact, while in lap shear connections, single or double-sided, the holes are always confined out of plane, in case of connections with long bolts and gusset plates (typical of tubular structures), the holes are constrained out of plane outwards, but they are free to buckle inwards, providing a reduction of the bearing strength. Within this framework, the paper is aimed at the development of an analytical formulation for the prediction of the bearing resistance of connections with long bolts and square hollow sections (SHS). The proposal is based on the calculation of the post-buckling load of the tube's plate subjected to the bearing at the bolt's hole, combining the Winter's formula (originally developed to predict the post-buckling strength of steel plates accounting for geometrical and mechanical imperfections) with a simplified FE model developed in SAP 2000. The procedure developed is presented in detail proposing a design equation for connections with long bolts, based on a formula suggested recently by Može (2014, 2016) suitable for the inclusion in code provisions such as EC3. The accuracy of the design equation is checked on the experimental data reported in a previous work of the same authors properly extended with parametric FE simulations to cope for variation of geometrical parameters.

Keywords: Bearing resistance, Buckling, SHS, Shear, Model, Eurocode 3

x Corresponding author

1. Introduction

Bolted connections are widely used in steelwork because they are easy to manufacture while providing significant benefits in terms of constructability. In fact, they allow to split complex structures in simpler parts which can be welded in the shop (assuring a high quality of welds) and bolted on the construction site. Almost all bolted connections, in order to provide an appropriate response, need to activate the typical mechanisms for the transfer of shear forces, thus requiring to check resistance accounting for different possible failure modes. In the most elementary type of connections, plates are simply overlapped according to single-sided or double-sided lap shear configurations, providing the load transfer through the activation of bearing stresses and shear forces in plate and bolt. The bearing stresses develop in the area of the plate ahead of the bolt shank and, usually, due to a combination of material strain hardening and stress triaxiality, they achieve levels much beyond the yield limit of steel [1-3]. In order to account for this triaxial stress state, promoted by the lateral confinement of the bolt head or nut, currently, all the national and international codes suggest to adopt an average value of the bearing stress which is likely to achieve, depending on the level of confinement, up to four times the ultimate resistance (f_u) of the base material [4-6].

In case of classical double-sided and single-sided lap shear connections, the bearing strength has been extensively investigated over the last twenty years both for standard and Cold-Formed Steelwork (CFS). However, if reference is made, as an example, to the European (Eurocode 3 part 1.8 [4] and Eurocode 3 part 1.3 [5]) and North-American design codes (AISC 360-10 [7] and AISI S100 [6]), many differences, mainly related to the background documentation followed to develop the standardized design procedures can be still recognized. Generally, it is common practice to merge in the same formula the checks for the so-called bearing and tear-out failure modes, expressing the bearing resistance at the bolt hole as the product of an average bearing stress multiplied by the bearing area. Despite this, even though the equation is expressed in this way in all the most widespread standards, the definition of the design bearing factors does not find a common agreement. As an example, in AISI S100 the bearing stress may range, in case of standard holes, from $1.35f_u$ (for very thin plates and minimum confinement) to $4f_u$ (for thick plates and maximum confinement). Differently, but with a similar equation, AISC 360-10 limits the average bearing stress to an upper bound value of $3f_u$. Conversely, in European practice, Eurocode 3 part 1.8 limits the bearing factor to a maximum value equal to $2.5f_u$ being, therefore, much more conservative than all the other design provisions. This lack of consistence between the various design provisions has already been evidenced by several authors (e.g. [2, 8, 9]). Though, the definition of a unique and commonly accepted criterion is still far from being achieved. In the European framework, the most recent proposals are those provided by the research group of the University of Ljubljana that, in a series of works published since 2010 [1-3], has

suggested a more accurate procedure for the European practice, developing a new equation validated on a large sample of experiments including mild and high strength steels. This new formula considers the possibility to achieve an average bearing stress equal to $3f_u$, limited, eventually, by the development of tear-out failure modes, which are accounted for with an approach very similar to that reported in one of the earlier versions of the AISC, (1993) specification [9,10]. Examples of other recent works, which underline the continuous need for more accurate design procedures, as well as the complexity of the topic, are those of Salih et al. [11], Kim & Kuwamura [12] and Kymaz [13] regarding the behavior of bearing in stainless steel connections, Draganic et al. [8] or Teh & Uz [14] dealing with single sided connections, the series of works by Teh and coauthors [14-17] or other recent experimental works [18-24].

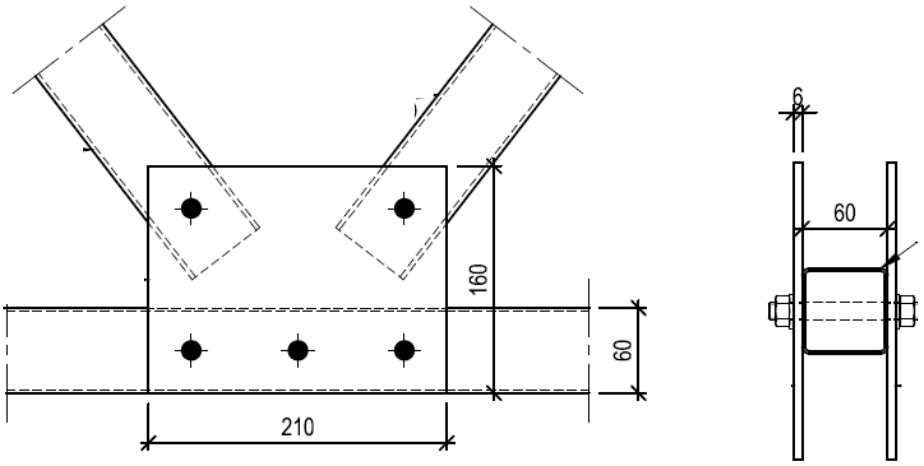

Fig. 1 – Example of a typical configuration of a joint with tubular elements, gusset plates and long bolts

As herein described, the technical literature regarding the bearing resistance at bolt holes is very wide. Though, it is practically exclusively devoted to sheet-to-sheet connections in double-sided or single-sided configurations, almost completely disregarding other possible configurations, such as the case of connections with long bolts fastening structural elements with a gap (e.g. hollow sections, channels or simply spaced gusset plates). However, even in absence of regulations and specific experimental works, such a kind of connections are widely used in constructions, in CFS assemblies and ordinary steelwork, for trusses, racking systems, bracings, scaffoldings, etc. (Fig.1). Indeed, at the author's best knowledge, currently the only explicit specification in design standards for this connection typology is that reported in AISC 360-10 [7] (Equation J7-1), while there are only very few theoretical and experimental works, such as that of Yu & Panyanouvong [25].

The main difference between a traditional sheet-to-sheet connection and a connection with long bolts passing completely through the member is that due to the lack of installation space, the bolt head or nut can confine the plates subjected to bearing only outwards, while inwards they are free to buckle (Fig.2). Clearly, compared to the classical overlapped configurations, this leads to a strong decrease of

the confinement, thus reducing the value of the maximum achievable bearing stress. In fact, as already evidenced in [26], in many cases, in this type of connection, due to the development of a particular out-of-plane failure mode of the plate, the bearing stresses cannot attain values as high as those reported neither in the recent proposal of Može [3] (i.e. $3f_u$) nor in the AISI S100 or EC3 provisions (i.e. $2.25f_u$ [26] or $2.5f_u$ [4,5]) .

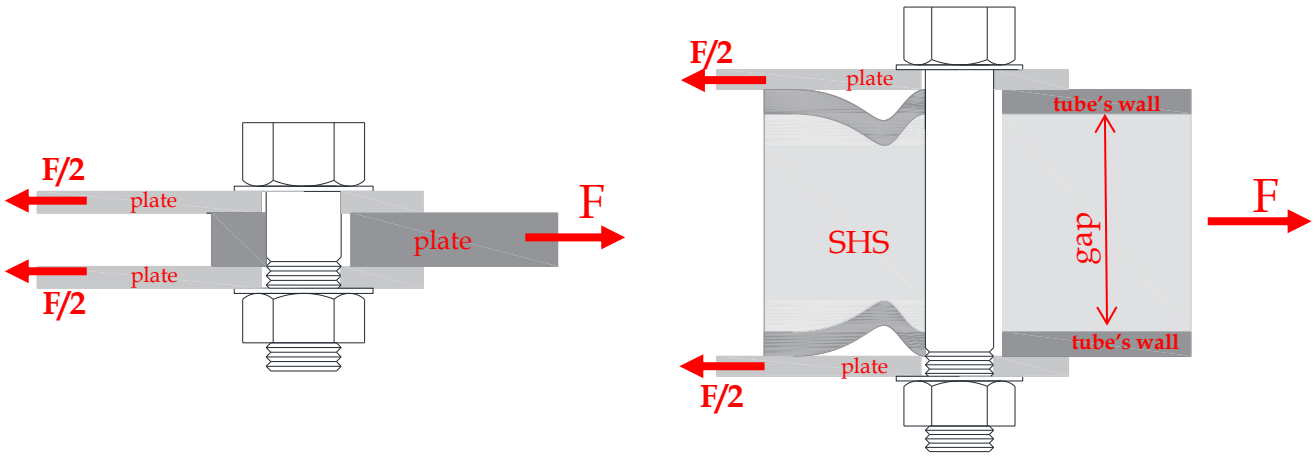

a) Sheet-to-sheet connection (full lateral confinement)

b) Connection with a gap (confinement only on one side)

Fig. 2 – Different confinement's effect in sheet-to-sheet and connections with a gap

Within this framework, aiming to provide a contribution towards the development of specific design guidelines for connections composed by gusset plates, squared hollow sections and long bolts, the main goal of this paper is to investigate the behaviour of this joint typology, with the aim of providing an analytical formula able to predict the bearing strength at bolt holes, introducing in the recent proposal for revision of Eurocode 3 made by Može et al. [2-3] a further check to be considered in the case of connections with long bolts and Squared Hollow Sections (SHS). The new analytical formulation is based on the calculation of the post-buckling load of the tube's plate subjected to the bearing action of the bolt, combining the Winter's equation [27] (originally developed to predict the post-buckling strength of steel plates under compression, accounting for geometrical and mechanical imperfections) with a simplified FE model developed in SAP 2000 [28]. This model is used to determine the elastic buckling load for the particular loading condition (patch load with partial rigidity constraints) which, otherwise, would be quite complex in a closed form. The procedure developed is presented in detail proposing a design equation whose accuracy is checked on the experimental data reported in a previous work of the same authors properly extended with parametric FE simulations [26]. The additional FE analyses are carried out in order to consider the variation of the main geometrical parameters influencing the bearing resistance.

2. Current design practice for bearing strength at bolt holes

In order to clarify what are the approaches proposed in the most recent codes for the prediction of the bearing resistance at bolt holes, in the following the main suggestions currently available are summarized.

The AISI S100 code is essentially based on the works of Yu, Zadanfarrokh & Bryan, LaBoube & Yu, Wallace, Schuster and LaBoube and Rogers & Hancock [29-41]. In particular, Rogers & Hancock first and Wallace, Schuster and LaBoube after, conducted tests on CFS bolted connections defining, as it is practically made in all the codes, the bearing strength as dependent on the tensile strength of the plate (f_u), thickness of the sheet (t) and bolt diameter (d). Additionally, the authors after verification with a database including various research reports, expressed the stress bearing coefficient as the product of a modification factor m_f (dependent on the connection typology and, specifically, on the level of lateral confinement of the hole in bearing), multiplied by a bearing factor C dependent, in turn, on the t/d ratio. The product of these two coefficients may lead, for connections with standard holes, to values of the bearing stress ranging from a minimum of $1.35f_u$ (d/t>22, single-sided or outside sheet of a double shear connection without washers or only one washer) to a maximum of $4f_u$ (d/t<10, inside sheet of double shear connection with or without washers):

$$F_b = Cm_f f_u t d \ ^* \tag{1}$$

AISI S100

$$C = 3 \quad for \frac{d}{t} \leq 10 - \ C = 4 - 0.1\ \frac{d}{t} \quad for \frac{d}{t} \leq 22 \ / \ C = 1.8 \quad for \frac{d}{t} > 22^{**} \tag{2}$$

**modification factors reported in Table J3.3.1-2 of AISI S100 (0.75<m_f<1.33 for standard holes)*

*** values for connections with standard holes*

Furthermore, with a very advanced approach, AISI S100 proposes also a reduced value of the bearing strength to be used only in the load combinations where the bolts' holes deformation is a design consideration expressing, eventually, the need to limit deformations at bolt holes under service load conditions. Practically, the same design procedures given in AISI S100 are reported also in the Australian and New Zealand Standard AS/NZS 4600:2005 [42] for CFS, whose background documents are mainly the works of Rogers & Hancock [34-41].

AISC 360-10 neglects the dependence on the t/d ratio and the influence of the connection typology, but provides a similar design equation expressing the bearing strength as equal to 1.2 or 1.5 times the clear distance in the bolt's force direction (l_c) multiplied by the plate thickness and ultimate stress of the material (F_u), with a limitation to the maximum achievable bearing stress equal to $2.4F_u$ or $3F_u$. Also in this case, the alternative choice of the factors 1.2 or 1.5 and 2.4 or 3, depends on whether the deformation at bolt holes is or it is not a design consideration:

AISC 360-10

(normal connections in standard holes)

$$F_b = 1.5 l_c t F_u < 3 d t F_u \ * \quad (3)$$

$$F_b = 1.2 l_c t F_u < 2.4 d t F_u \ ** \quad (4)$$

** if the bolt hole deformation is not a design consideration*

*** if the bolt hole deformation is a design consideration at service loads*

Additionally, for connections made using bolts that pass completely through an unstiffened box member or HSS, AISC 360-10 suggests to make reference to the equation normally used for pins in bearing, expressing the bearing strength as the area in bearing (A_{pb}) multiplied by 1.8 times the nominal yield stress (F_y):

AISC 360-10

(connections in HSS members)

$$F_b = 1.8 F_y A_{pb} < 1.5 l_c t F_u < 3 d t F_u \quad (5)$$

In European practice the current rules for connections in normal steelwork and CFS are those contained in Eurocode 3 part 1.8 and part 1.3 respectively [4,5], whose background is based on the work done at the end of the 80s' by one of the working groups for the Eurocodes [43-45] which, at the time, provided a synthesis of the most recent experiences of those ages. On the base of these analyses a model covering the basic failure modes delivered in Fig.3 was developed. The equations reported in the Eurocodes are very similar to the design formulas of AISC 360 but, in truth, more conservative and more complicated due to the introduction of a dependence between the bearing factor and the distance of the hole center from the lateral edge (e_2).

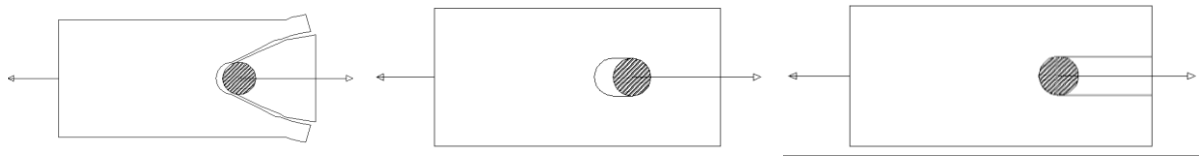

(a) ***(b)*** ***(c)***

Fig. 3 –Splitting failure (a), Bearing Failure (b), Tear-out failure(c).

The dependence of the bearing factor on e_2, expressed by the k coefficient, as already evidenced by Može et al [2] was included in the formula due to the lack of experimental evidence and is relevant only when e_2 is lower than $1.5 d_0$. Practically it adds a check for the splitting failure mode (Fig.3a) and a check of the holed section of the plate in tension, which is in any case covered in the Eurocode by a specific check of the net cross-section resistance:

Eurocode 3 part 1.8

(connections joining plates starting from a

$$F_b = k \alpha f_u t d \ *$$

$$\alpha = min\left(\frac{e_1}{3 d_0}; \frac{f_{ub}}{f_u}; 1\right) \text{ for end bolts} \quad (6)$$

thickness of 4 mm)

$$\alpha = min\left(\frac{p_1}{3d_0} - \frac{3}{4}; \frac{f_{ub}}{f_u}; 1\right) \text{ for inner bolts}$$

$$k = min\left(2.8\frac{e_2}{d_0} - 1.7; 2.5\right) \text{ for edge bolts}$$

$$k = min\left(1.4\frac{p_2}{d_0} - 1.7; 2.5\right) \text{ for inner bolts}$$

* with:
e_1= distance from the edge in the direction of the force (end distance)
e_2= distance from the edge orthogonally to the force (edge distance)
p_1= spacing in the direction of the force
p_2= spacing orthogonally to the force
d_0= diameter of the bolt's hole

In Eurocode 3 part 1.3, an equation with the same structure of part 1.8 is suggested, but the dependence of the bearing resistance on the plate thickness is introduced with a coefficient k_t, correcting the resistance given by Eq.(6) while assuming a value of k equal to 2.5:

Eurocode 3 part 1.3
(connections joining plates with 1.25 mm<t<4 mm)

$$F_b = 2.5k_t\alpha f_u t d$$

$$k_t = \frac{(0.8t + 1.5)}{2.5} \quad for\ 0.75\ mm \le t \le 1.25\ mm; \qquad (7)$$

$$k_t = 1 \quad for\ t > 1.25\ mm$$

From the review of the code provisions previously reported it is clear that the only design equation specifically devoted to the case of long bolts passing through a section with a gap is that proposed by AISC 360-10, namely Eq.(5). Conversely, all the other formulas herein reported are not specifically referred to the case of long bolts and therefore they should not be blindly extended because of the risk to get to unsafe predictions. In fact, in a previous work of the same authors a preliminary investigation dealing with the accuracy of current code formulations was performed, demonstrating that the equations formerly given are not able to provide a satisfactory prediction of the actual connection behaviour [26]. Indeed, for connections made with Squared Hollow Sections (SHS), gusset plates and long bolts, it was already shown in [26] that Eurocode 3 provides conservative results in the range of high plate thicknesses (*t>4mm*) while providing unsafe predictions for low plate thicknesses (*t<4mm*). Conversely, AISI S100, accounting more accurately for the dependence on the *t/d* ratio, provides a better approximation for lower thicknesses assuming a modification factor equal to 0.75 but in any case, as it is not specifically calibrated for the case of long bolts, still provides a significant overestimation of the resistance in many cases. Similarly, also the provisions of AISC 360-10 are not accurate and in fact, Eqs.(3-4) lead in general to an overestimation of the resistance, while, Eq.(5) provides a significant underestimation.

This preliminary review justifies the work hereinafter reported, considering the need for the definition of design rules more specifically devoted to the case of long bolts. As above said, the model presented afterwards follows the proposal recently made in view of a new Eurocode standard by Može [2,3],

introducing a further check for the plate's buckling to be considered only in case of connections with long bolts and a gap. In particular, the analysis reported in the next sections is specifically devoted to a very common case which is that of connections made up of gusset plates and SHS members. Anyway, the same methodology hereinafter presented could be applied to extend the approach also to other joint configurations with long bolts. As it will be used for the calibration of the equation reported afterwards, the recent proposal of Može [2,3] is herein recalled. It simply regards an update of the EC3 part 1.8 formula in which the bearing strength, consistently with other international codes, can assume a maximum value equal to 3. Furthermore, in view of a simplification, the coefficient k is removed, while a correction factor (k_b) accounting for the steel grade is introduced:

Može [2,3]

$$
\begin{aligned}
&F_b = k_b \alpha f_u t d \\
&\alpha = min\left(\frac{e_1}{d_0};\ 3\right) \textit{ for end bolts} \\
&\alpha = min\left(\frac{p_1}{d_0} - \frac{1}{4};\ 3\right) \textit{ for inner bolts} \\
&k = 1 \textit{ for steel grades lower than S460} \\
&k = 0.9 \textit{ for steel grades higher or equal to S460}
\end{aligned}
\tag{8}
$$

It is worth noting that in the original works of Može [2,3] it is indicated that the bearing factor, for a single bolted connection, in general, can achieve a maximum stress even equal to $5f_u$. Nevertheless, a reduction of the bearing coefficient to 3 is suggested by the same author to introduce, indirectly, a control on the development of brittle failure modes.

3. Main outcomes of the previous activity [26]

In order to evaluate the behavior of connections with long bolts passing through tubular members subjected to shear forces, an experimental programme regarding 24 specimens was performed at the Laboratory for Materials and Structures of the University of Liège (Fig.4) [26].

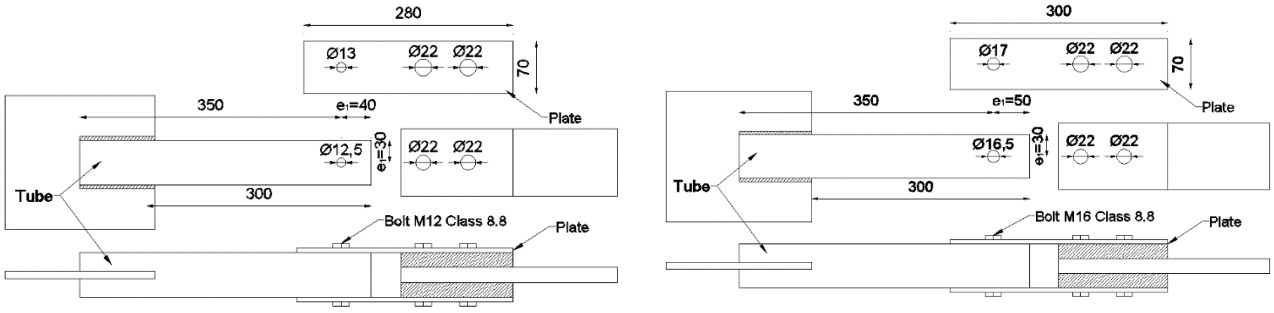

a) SHS 70x70mm with M12 bolts, thickness equal to 2, 2.5 or 4 mm and steel S235 or HX420LAD

b) SHS 70x70 mm with M16 bolts, thickness equal to 2, 2.5 or 4 mm and steel S235 or HX420LAD

Fig. 4 – Specimens' typologies examined in [26]

The results of this experimental work, which was followed also by the development of a FE model in ABAQUS and further parametric analyses to cope for variation of geometrical properties, are reported in detail in [26] and are hereinafter recalled just to summarize the main outcomes of this activity, which is the main reference for the further developments described in this paper. The specimens consisted in elementary connections made up of tubular SHS members fastened with external gusset plates and with a single long bolt, subjected to tensile axial forces in order to generate a shear in the connection (Fig.4). The specimens were realized both with S235 and HX420LAD steel, considering three different tubes' wall thicknesses, namely 2, 2.5 and 4 mm and two bolts' diameters (M12 and M16). For every considered combination of steel grade, tube's thickness and bolt diameter, four nominally equal specimens were tested.

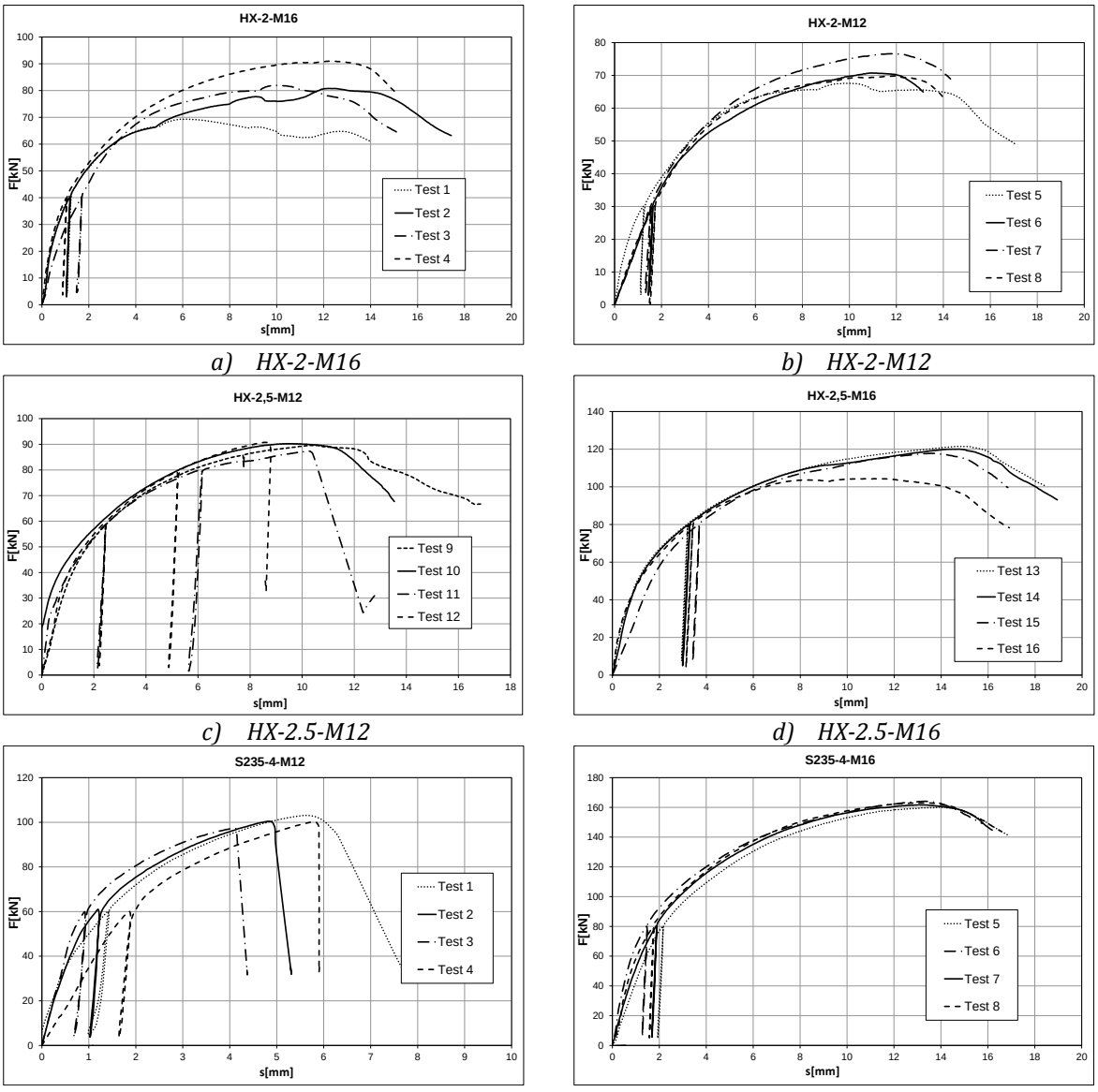

a) HX-2-M16 *b) HX-2-M12*

c) HX-2.5-M12 *d) HX-2.5-M16*

e) S235-4-M12 *f) S235-4-M16*

Fig. 5 – Experimental Force-Displacement curves [26]

206 The tests, whose results are summarized in Figs.5, showed a response that was similar for all the
207 specimens in terms of force-displacement, distinguishing only the cases where the bolt's failure was
208 prominent, whose response was characterized by the achievement of the maximum resistance and
209 then by a sudden drop (e.g. Fig.5e), from the cases where the hole's failure was observed, whose
210 response was more ductile and characterized by the development of a smooth softening branch after
211 the attainment of the peak force (e.g. Fig.5f) (the labels reported in the graphs' titles of Figs.5 identify
212 the steel grade (HX which stands for HX420LAD or S235), the tube's thickness (2, 2.5 or 4 mm) and the
213 bolt diameter (M12 or M16)).

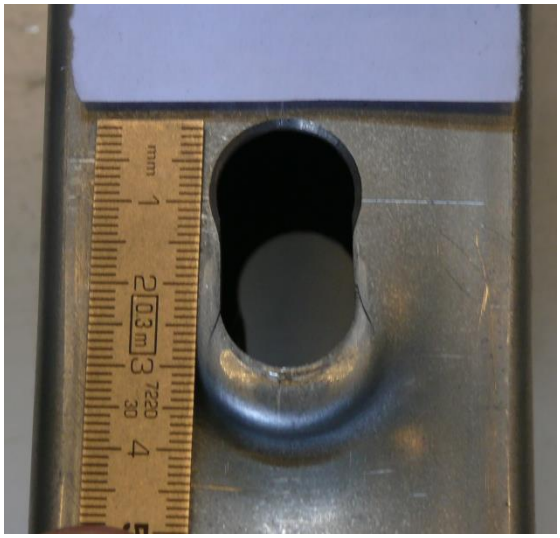

a) Local buckling failure at the bolt's hole (Test HX-2-M16)

b) Local buckling failure at the bolt's hole, particular of the bump (Test HX-2-M16)

c) Tear-out failure (Test S235-4-M16)

d) Bolt's failure (Test S235-4-M12)

214 **Fig. 6 –** Typical failure modes observed in the tests reported in [26]

Even though the shape of the force-displacement curves for all the specimens was in line with the expectations, the observed failure modes were very peculiar, identifying the development of a new failure mechanism, which is normally not accounted for in traditional design equations. Indeed, in cases with high strength steel (HX420LAD grade) and low thickness of the SHS tube (equal to 2 and 2.5 mm) a failure mode characterized by the development of local bumps in the bearing area ahead the bolt's shank was observed (Figs.6a,b). Conversely, in all the other tests with higher tube thickness, due to the lower local slenderness of the tube's hole under bearing (higher thickness over bolt's diameter ratio) the traditional failure modes were identified, namely tear-out, bearing or shear failure of the bolt's shank (Figs.6c,d).

The experimental results, that gave mainly a first phenomenological observation, were used to calibrate a FE model in ABAQUS extending the experimental sample with further analyses devoted to consider other geometries. Subsequently, all the data collected, experimental and simulated, were used to verify the accuracy of the currently available equations (see section 2) evidencing the need for a more accurate formulation able to predict the bearing resistance in case of connections with long bolts and members with a gap, accounting also for the possible development of local buckling phenomena at the bolt holes, such as those observed in the experiments. Indeed, the comparison of the experimental and FE results with the EC3 and AISI S100 formulations reported in [26] evidenced that the codified models are not able to predict accurately the connection's resistance, even though the application of AISI S100 equations with the minimum value of the modification factor allowed for standard holes (m_f=0.75) provides a safe prediction and a better approximation at least in the low thickness over bolt diameter ratio range (Fig.7). In all the other cases both EC3 part 1.3 or 1.8 and AISI S100 specification do not seem accurate.

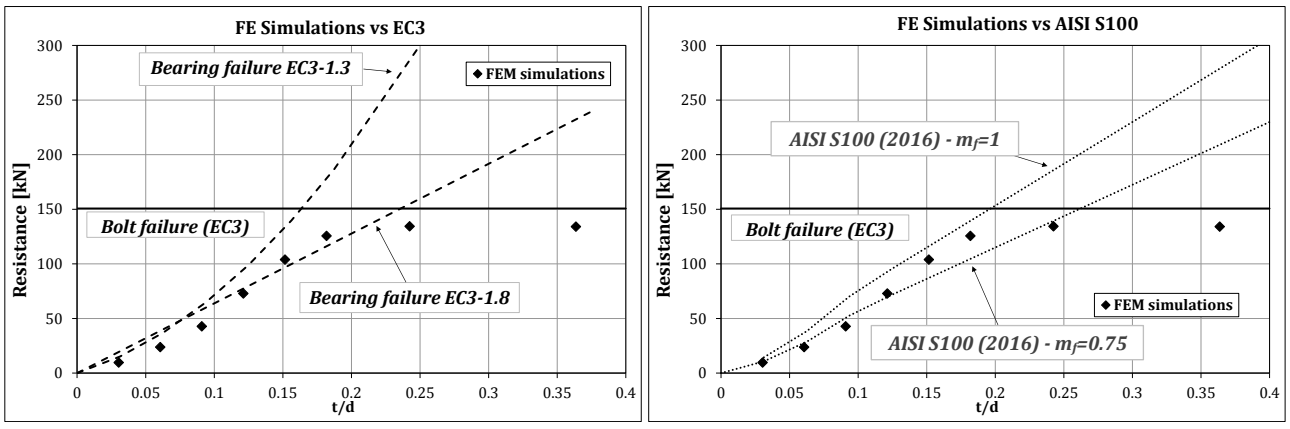

Fig. 7 – Accuracy of EC3 and AISI S100 equations

4 Prediction of the critical buckling load for unconfined bolt holes under bearing

This section is devoted to the definition of a procedure to evaluate the post-elastic buckling load of connections of a SHS tube with through-all long bolts. The knowledge of such a buckling load value is necessary in order to account in design for the particular failure mode that was observed in the experiments reported in [26], previously briefly described (Figs.6a,b). The prediction of the post-elastic failure load, with the approach described afterwards in this section, is meant to introduce in the recent equation proposed by Može et al. [2-3] (validated for standard lap shear connections) a further check for local buckling to be considered only in case of connections with long bolts and Squared Hollow Sections (SHS), where this particular failure mode can actually develop. The Može et al. model [2-3] is selected because it was already demonstrated to be more simple and more accurate than EC3 model and, additionally, it has already been calibrated in view of the definition of a new standard for the European practice. As aforesaid, the new analytical formulation is developed combining Winter's equation [27] with a FE model developed in SAP 2000 [28]. The purpose of the FE model is to provide a prediction of the elastic buckling load (necessary to apply Winter's equation) which otherwise, for the particular loading and restraining conditions would be very complex in a closed form. Therefore, in the following the procedure adopted to define the elastic critical buckling load is described in detail and, afterwards the Winter's approach is applied in order to account for geometrical and mechanical non-linearities. Subsequently, by means of a parametric analysis a simple design equation expressed as a function of the main geometrical parameters of the connection under investigation is calibrated through regression analysis of simulated data. The details of the procedure are hereinafter reported.

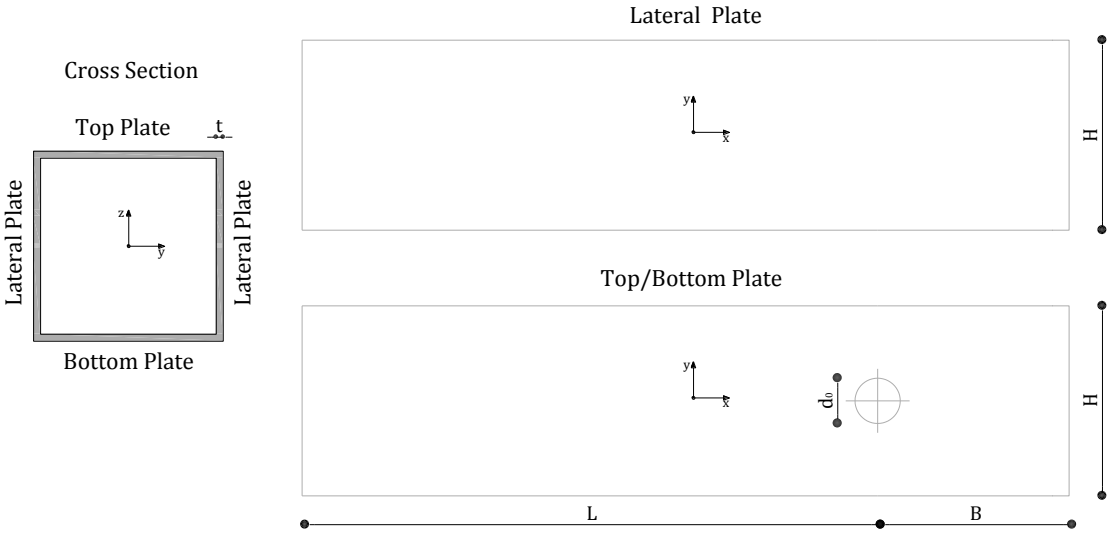

Fig. 8 – Scheme of the analysed connection

4.1 Evaluation of the elastic and post-elastic buckling load

The procedure applied in this work to assess the value of the elastic critical load leading to the local buckling of the tube's hole is carried out starting from the analysis of a very simple sub-structure extracted from the whole connection representative of the zone where the local buckling effects are more significant. In particular, in view of simplification, the sub-structure is idealized extracting from the tube only the end part of the plate directly loaded from the bolt's force, whose dimensions are the width of the tube (H) and the distance between the centre of the hole and the free edge of the tube (e_1) (Fig.8). This is the zone that, as also demonstrated by the experimental analysis, is more significantly affected by the local buckling phenomena.

Dealing with the modelling of buckling phenomena, it is well known that the definition of the restraining conditions applied at the edges of the plate is of paramount importance, due to the influence that the constraints have on the value of the critical buckling load. This is the reason why, even though in the present work only a small portion of the tube is studied, the continuity of the analysed plate with the remaining parts of the tube is recovered by considering appropriate boundary conditions applied on the edges of the element (Fig.9).

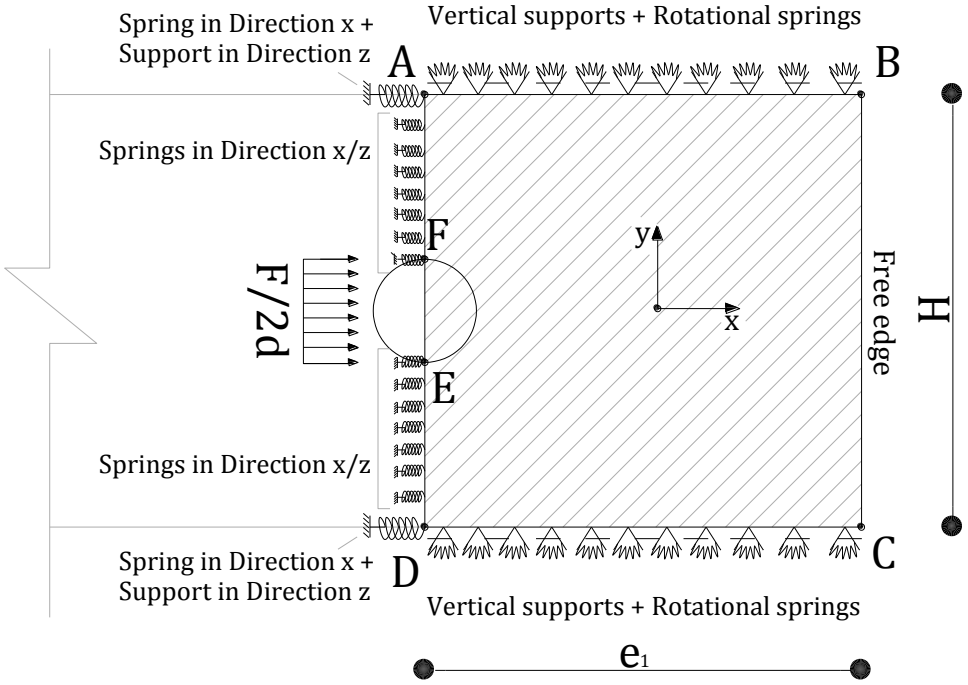

Fig. 9 - Boundary conditions

In particular, in the following, the considerations made to define the stiffness of appropriate springs able to account for the rotational, shear and axial behaviour of the remaining parts of the tube's plates

are described. In particular, in order to account for the remaining portions of the tube the following constraints are applied at the edges of the analysed plate (Fig.9):

- at the intersection of the edges of the plate with the lateral walls of the tube rotational springs and vertical supports are applied (edges A-B and D-C);
- on the edge loaded under compression by the bolt, in-plane and out-of-plane springs are introduced both on the portions of the edge next to the hole (edges A-F and D-E) and in the corners of the plate (points A and D). Furthermore, in the zone of the hole, a uniform load modelling the shear action transferred by the bolt is introduced;
- at the free edge of the tube no boundary conditions are introduced (edge B-C);

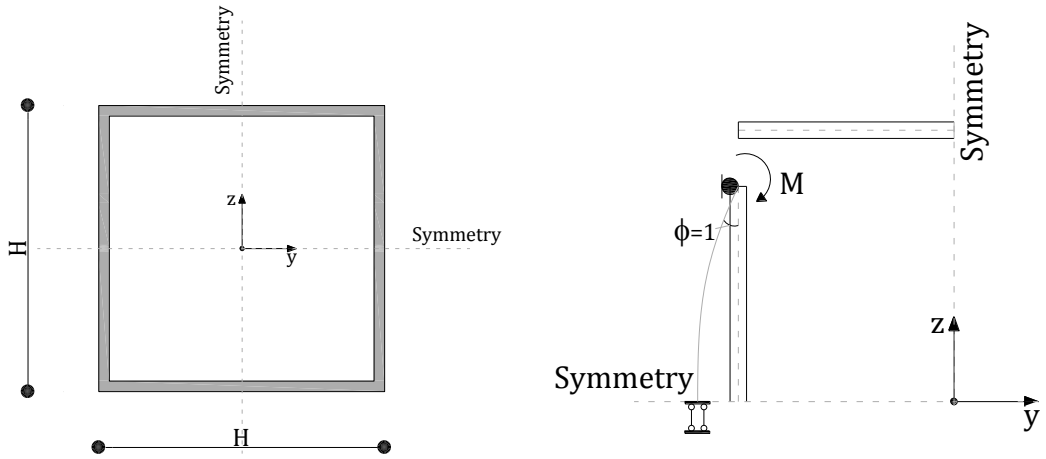

Fig. 10 – Scheme used to define the rotational stiffness due to the lateral plates of the tube

Therefore, on the ***sides of the plate parallel to the load*** (from A to B and from D to C, fig. 9), out-of-plane supports and rotational springs are applied in order to model the axial and rotational stiffness of the lateral plates of the tube. In particular, in order to model the axial stiffness of the lateral plates of the tube, on these edges, the out-of-plane supports are defined as rigid elements. Conversely, the stiffness of the rotational springs is determined by defining the value of the bending moment needed to generate a unitary rotation on the lateral plates of the tube (Fig.11). By adopting this approach, the following expression is obtained:

$$k_{\phi,lateral} = \frac{2EI}{H} \tag{9}$$

where E is the modulus of elasticity of steel, I is the moment of inertia of the lateral tube's plate per unit of length and H is the height of the tube's plate.

The ***side that goes from B to C*** is considered free; a similar assumption is made for the portion of the edge on which the load is applied that goes from E to F. In addition, to take into account for the

stiffness of the remaining part of the tube behind the analysed plate, various considerations are made. In particular, at points A and D of the model (***the corners of the plate***) extensional springs in the *x* direction accounting for the stiffness of the portion of the lateral plate behind the bolt are applied. The stiffness of such springs is easily calculated as:

$$k_{x,corners} = \frac{E(A_{lp}/2)}{L} \tag{10}$$

where *L* is the length of the tube and A_{lw} is the area of the lateral wall of tube calculated as the product of the tube thickness *t* and *H/2*. In the same way, in the ***zone going from A to F and from E to D*** extensional springs are spread along the edges both in the *x* and in the *y* direction. As already made for the stiffness $k_{x,corners}$, the value of the stiffness of the springs spread on the loaded edge is determined in order to account for the axial deformability of the remaining part of the top plate located behind the bolt:

$$k_{x,edge} = \frac{E(A_{tp}/2)}{L} \tag{11}$$

where A_{tp} is the area of the top plate of the tube calculated as the product of the tube thickness *t* and *H*. Conversely, the stiffness of the springs in the *y* direction is determined in order to account for the out-of-plane deformability of the portion of the tube behind the bolt hole. To this scope, the simple scheme of plate fully restrained on three edges loaded with a unitary force applied on the free edge represented in Fig.11 has been studied. Therefore, in order to determine the value of the stiffness of the springs to be applied on the holed side of the plate several schemes with the force applied in different points of the free edge have been solved.

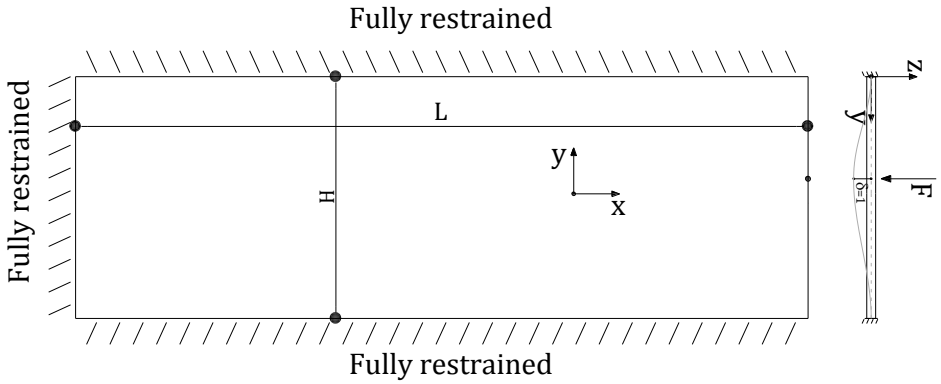

Fig. 11 – Scheme used to evaluate the out-of-plane stiffness of the springs applied on the holed edge

The result of this analysis is delivered in Fig. 12 where the value of the generic spring stiffness is represented versus the distance of the point of application of the force from the mid-point of the edge. From such a figure it is possible to observe that the out-of-plane stiffness of the plate is almost

constant in the central area, while in the end regions it asymptotically tends to infinity due to the presence of the full restraints. In order to maintain a simple structure of the model and to avoid to introduce a variable value of the springs' stiffness, the out-of-plane stiffness of the springs has been assumed constant and equal to the value of the force needed to obtain a unitary displacement at the mid-point of the plate's edge. Conversely, at the corners of the plate, as already said, a fixed support has been applied. This choice is justified by the fact that, from some preliminary analyses, no appreciable differences were found in the results considering a variable value of the springs' stiffness or a constant value.

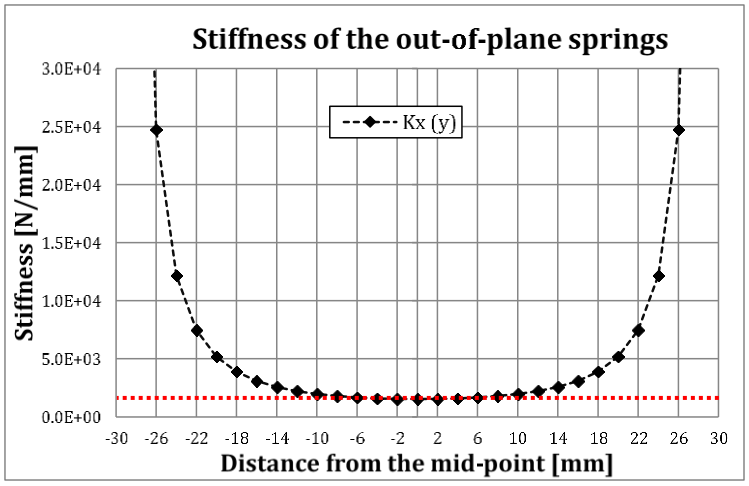

Fig. 12 – Stiffness for out-of-plane springs

Under the reported hypotheses, the value of the elastic buckling load of the plate with the above described boundary conditions has been determined by developing an appropriate FE model in SAP2000 v.16 software package. The model has been developed by means of the following steps: geometrical characterization of the plate, definition of the material properties, definition of the boundary conditions and choice of the elements and size of the mesh. The geometry of the plate has been defined by using the automatic tools provided by the software, which are able to generate and to partition in a very simple way the plate, after defining the dimensions and the number of divisions of the elements. The plate section has been provided by introducing in the model the thickness of the plate and by choosing the shell formulation. In particular, in the proposed FE model the so-called "thin-shell" formulation has been used, i.e. a shell formulation following the Kirchhoff model [46], where the transverse shear deformations are neglected. Due to the typical aspect ratio and thickness of the analysed plates, this is considered a reasonable hypothesis. The material properties of the steel plate have been simply described by means of an elastic isotropic model with elastic modulus equal to 210.000 MPa and Poisson's ratio equal to 0.3. The optimal mesh subdivision has been defined after performing several preliminary analyses devoted to investigate the dependence of the result from the

mesh size. After these preliminary analyses a minimum dimension of the area element equal to 2.5 mm x 2.5 mm has been chosen (Fig.13).

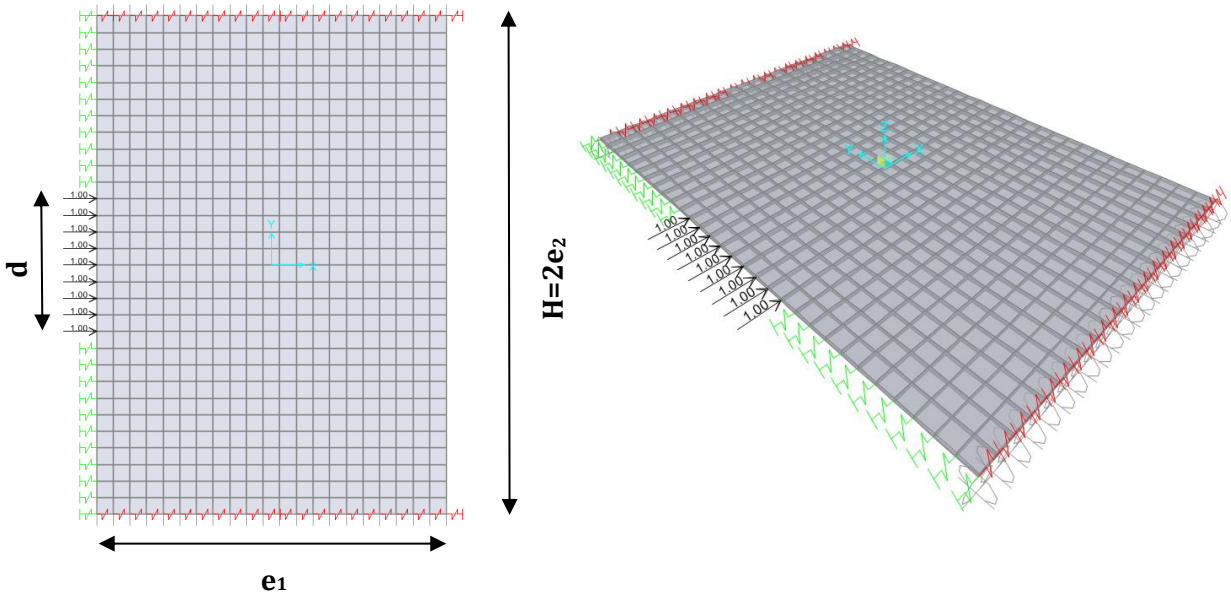

Fig. 13 – SAP2000 model of the plate

An example of the results of one of the analyses presented in the next section is delivered in Fig.14, where the shapes of the first four buckling modes of one on the analysed cases are represented. As it is possible to verify, the 1st buckling shape, i.e the buckling shape characterized by the lowest value of the load multiplier, is the one typically observed also in the experimental analysis.

e_1=48 mm, H=60 mm, t = 0.50 mm, d=16 mm

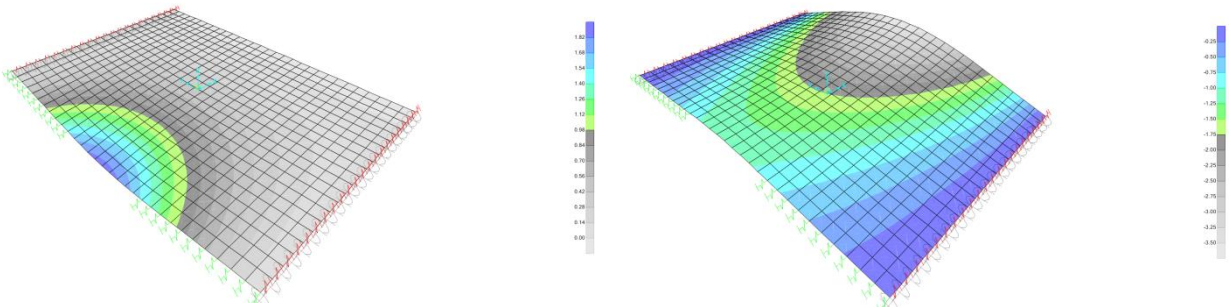

1st mode – α_{cr}=105.3

2nd mode – α_{cr}=306.8

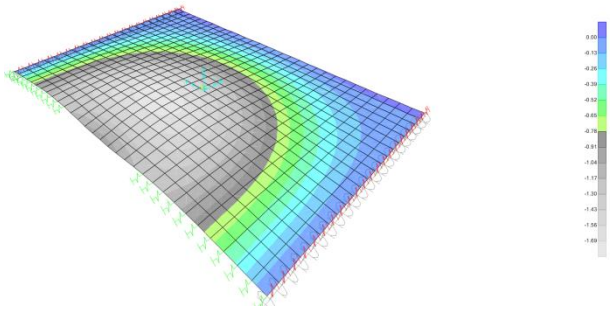

3rd mode – α_{cr}=441.1

Fig. 14 – Buckling modes for a plate with thickness equal to 0.50 mm

After determining the elastic buckling load, in order to obtain the actual value of the ultimate buckling load it is necessary to account for two additional parameters that normally provide a significant influence: the imperfections and the non-linear behaviour of steel. In fact, both these factors, as widely recognized in technical literature, may provide a significant variation to the value of the buckling resistance calculated by means of an elastic analysis and, therefore, they need to be properly accounted for. In this work, in order to account for these factors, the empirical approach of Winter [27], already proposed by EC3 and by the AISI specification, is followed in order to account for the influence of imperfections and of the non-linear behaviour of the material. Such an approach, on which the effective width concept is based, provides to correct the value of the ultimate load that the plate can carry by means of the following expression:

$$N_{cr,pe} = N_{pl}\rho = N_{pl}\left[\left(1 - \frac{0{,}22}{\overline{\lambda_p}}\right)\frac{1}{\overline{\lambda_p}}\right] \leq N_{pl} \tag{12}$$

where $\overline{\lambda_p}$ is the non-dimensional slenderness parameter expressed as:

$$\overline{\lambda_p} = \left(\frac{N_{pl}}{F_{cr,el}}\right)^{1/2} \tag{13}$$

where $F_{cr,el}$ is the value of the elastic buckling load, evaluated in this work by means of the buckling analyses described previously, and N_{pl} is the value of the plastic load. It is worth noting that, according to the Winter's methodology, the two coefficients $\frac{1}{\overline{\lambda_p}}$ and $\left(1 - \frac{0{,}22}{\overline{\lambda_p}}\right)$ reported in Eq.12 account for the influence of the mechanical non-linearity of the material and for the imperfections respectively [27,47]. The value of the plastic load N_{pl}, in the current case, can be determined following one of the approaches mentioned in section 2. In this work, the recent expression proposed by Može, namely

Eq.(8), is selected. This formulation, as demonstrated by the recent validation studies, is able to accurately predict the plastic resistance of a hole in bearing.

As far as the procedure to determine the critical buckling load at the bolt hole is defined (determination of the elastic buckling load by means of the SAP 2000 simple model previously described and of the post-elastic buckling load by means of the Winter's formula), in the next section, a parametric analysis is carried out in order to calibrate a simple design equation through regression analysis of a set of simulated data.

4.2 Calibration of a design equation

Basing on the procedure previously described, the aim of this section is to set up a simple design equation able to account for the buckling check in connections with SHS and trough-all long bolts. This can be made introducing in Eq.(8) a correction coefficient lower or equal to one accounting for the particular buckling failure mechanism arising in such a type of connections. In particular, with the aim to keep the same structure of the formulation proposed by Može, it is proposed to include in Eq.(8) an additional coefficient α_{st}, covering the buckling failure mode, calibrated by means of a parametric analysis performed applying the procedure previously described. Equating the ratio between the ultimate bearing resistance calculated according to Eq.(8) and the post-elastic buckling strength provided by Eq.(12), a new factor α_{st}, to be added in the bearing resistance formula of Može, can be easily defined:

$$\frac{F_b}{N_{cr,pe}} = \frac{F_b}{N_{pl}\rho} = \frac{\alpha_{st}(k\alpha dtf_u)}{(k\alpha dtf_u)\rho} = 1 \tag{14}$$

$$\alpha_{st} = \rho \tag{15}$$

where $\rho = \left(1 - \frac{0,22}{\overline{\lambda_p}}\right)\frac{1}{\overline{\lambda_p}} \leq 1$ is the buckling factor evaluated according to the Winter's formula (Eqs.12, 13).

Following this approach, in order to define a simple formula to be used in design, the main issue is to determine a correlation between ρ and the main geometrical parameters of the analysed connection. According to what reported in [26], the factors that influence the value of the ultimate load in case of buckling failure mode are t/d, e_1/d and e_2/d ratios. Therefore, the parametric study proposed in this section has been mainly devoted to investigate the influence of these three parameters on the value of ρ. To this scope, FE simulations have been performed by carrying out three groups of analyses according to the procedure previously defined, based on the determination of the elastic and post-elastic buckling load by means of the simplified SAP 2000 model and the Winter's formula. A ***first group*** of analyses devoted to check the influence of the t/d ratio. In this case the analyses have been carried out fixing the values of e_1/d equal to 3 and of e_2/d equal to 2.5 varying the bolt diameter d and

plate thickness t case by case. In particular, in this first group of analyses the values of d have been assumed equal to 12 and 16 mm and the t/d ratio has been varied in the range 0.05/0.15. The ***second group*** of analyses has been carried out in order to investigate the influence of the e_1/d ratio. In this case the analyses have been carried out by fixing the value of e_2/d equal to 2.5 and by varying t/d in between 0.1 and 0.3 and e_1/d in between 3 and 5. The ***third group*** of analyses has been carried out with the aim to investigate the dependence of the buckling resistance on the parameter e_2/d. In this case e_2/d has been varied in between 1.88 and 3.5, t/d has been varied in the range 0.03 and 0.15 and e_1/d has been fixed as equal to 3. For each of the considered combination of geometrical properties, the procedure previously reported to determine the value of the elastic and post-elastic buckling load has been applied and, subsequently, the values of the critical elastic buckling load and of the reduction factor calculated by means of the Winter's approach have been calculated. The results of these analyses are summarized in Tab.1.

Table 1 – *Results of the parametric analysis.*

1st group of analyses – influence of t/d												
t/d	***e_1/d***	***e_2/d***	***d [mm]***	***t [mm]***	***e_1 [mm]***	***e_2 [mm]***	***$N_{crit,elastic}$* [kN]***	***f_u** [MPa]***	***$N_{pl}= F_b$ [Eq.8] [kN]***	***λ_p [Eq.13]***	***ρ [Eq.13]***	***$N_{cr,pe}$ [Eq.12] [kN]***
0.05	3	2.5	16	0.8	48	40	3.51	499	18.58	2.30	0.39	7.30
0.075	3	2.5	16	1.2	48	40	11.84	499	27.87	1.53	0.56	15.56
0.1	3	2.5	16	1.6	48	40	28.08	499	37.16	1.15	0.70	26.13
0.125	3	2.5	16	2	48	40	54.84	499	46.45	0.92	0.83	38.41
0.15	3	2.5	16	2.4	48	40	94.77	499	55.74	0.77	0.93	51.83
0.05	3	2.5	12	0.6	36	30	1.86	499	10.35	2.36	0.38	3.98
0.075	3	2.5	12	0.9	36	30	6.30	499	15.52	1.57	0.55	8.50
0.1	3	2.5	12	1.2	36	30	14.95	499	20.69	1.18	0.69	14.30
0.125	3	2.5	12	1.5	36	30	29.20	499	25.87	0.94	0.81	21.06
0.15	3	2.5	12	1.8	36	30	50.46	499	31.04	0.78	0.92	28.48
2nd group of analyses – influence of e_1/d												
0.1	***3***	2.5	16	1.6	48	40	26.976	499	37.16	1.17	0.69	25.73
0.1	***3.5***	2.5	16	1.6	56	40	27.365	499	43.36	1.18	0.69	26.36
0.1	***4***	2.5	16	1.6	64	40	27.558	499	49.55	1.18	0.69	26.44
0.1	***4.5***	2.5	16	1.6	72	40	27.684	499	55.74	1.18	0.69	26.48
0.2	***3***	2.5	16	3.2	48	40	212.934	499	74.32	0.59	1.06	78.96
0.2	***3.5***	2.5	16	3.2	56	40	218.957	499	86.71	0.59	1.06	81.38
0.2	***4***	2.5	16	3.2	64	40	220.512	499	99.10	0.59	1.06	81.49
0.2	***4.5***	2.5	16	3.2	72	40	221.516	499	111.49	0.59	1.06	81.57
0.3	***3***	2.5	16	4.8	48	40	718.672	499	111.49	0.39	1.12	124.95
0.3	***3.5***	2.5	16	4.8	56	40	739.028	499	130.07	0.39	1.12	128.90
0.3	***4***	2.5	16	4.8	64	40	744.221	499	148.65	0.39	1.12	128.78
0.3	***4.5***	2.5	16	4.8	72	40	747.638	499	167.23	0.39	1.12	128.70
3rd group of analyses – influence of e_2/d												
0.031	3	***1.9***	16	0.5	48	30	0.948	499	11.61	3.50	0.27	3.11
0.063	3	***1.9***	16	1	48	30	7.59	499	23.23	1.75	0.50	11.61
0.094	3	***1.9***	16	1.5	48	30	25.59	499	34.84	1.17	0.70	24.23
0.125	3	***1.9***	16	2	48	30	60.69	499	46.45	0.87	0.86	39.74
0.16	3	***1.9***	16	2.5	48	30	118.53	499	58.07	0.70	0.98	56.88
0.0313	3	***2.5***	16	0.5	48	40	0.698	499	11.61	4.08	0.23	2.69

t/d	e_1/d	e_2/d	d [mm]	t [mm]	e_1 [mm]	e_2 [mm]	$N_{crit,elastic}$* [kN]	f_u** [MPa]	$N_{pl}= F_b$ [Eq.8] [kN]	λ_p [Eq.13]	ρ [Eq.13]	$N_{cr,pe}$ [Eq.12] [kN]
0.05	3	***2.5***	16	0.8	48	40	3.51	499	18.58	2.30	0.39	7.30
0.075	3	***2.5***	16	1.2	48	40	11.84	499	27.87	1.53	0.56	15.56
0.1	3	***2.5***	16	1.6	48	40	28.08	499	37.16	1.15	0.70	26.13
0.125	3	***2.5***	16	2	48	40	54.84	499	46.45	0.92	0.83	38.41
0.15	3	***2.5***	16	2.4	48	40	94.77	499	55.74	0.77	0.93	51.83
0.0313	3	***3.5***	16	0.5	48	56	0.51	499	11.61	4.77	0.20	2.32
0.05	3	***3.5***	16	0.8	48	56	2.402	499	18.58	2.78	0.33	6.15
0.075	3	***3.5***	16	1.2	48	56	7.115	499	27.87	1.98	0.45	12.52
0.1	3	***3.5***	16	1.6	48	56	16.774	499	37.16	1.49	0.57	21.28
0.125	3	***3.5***	16	2	48	56	32.77	499	46.45	1.19	0.68	31.81
0.15	3	***3.5***	16	2.4	48	56	56.62	499	55.74	0.99	0.78	43.72
0.05	3	***4.5***	16	0.8	48	72	1.651	499	18.58	3.35	0.28	5.18
0.075	3	***4.5***	16	1.2	48	72	5.908	499	27.87	2.17	0.41	11.53
0.1	3	***4.5***	16	1.6	48	72	13.209	499	37.16	1.68	0.52	19.25
0.125	3	***4.5***	16	2	48	72	25.820	499	46.45	1.34	0.62	28.95
0.15	3	***4.5***	16	2.4	48	72	44.617	499	55.74	1.12	0.72	40.05
0.2	3	***4.5***	16	3.2	48	72	105.766	499	74.32	0.84	0.88	65.39
0.225	3	***4.5***	16	3.6	48	72	150.584	499	83.61	0.75	0.95	79.08
0.25	3	***4.5***	16	4	50	72	206.493	499	96.78	0.68	0.99	95.23

*Calculated with the procedure reported in Section 3.1, namely by means of the FE model in SAP 2000

**Experimental data reported in [26]

As it is possible to verify from Table 1, the value of the elastic critical load shows a significant dependence on parameters t/d and e_2/d, while its dependence on e_1/d seems to be less significant. Furthermore, as demonstrated by the first group of analyses, the value of the reduction factor ρ calculated by means of the Winter's approach shows practically the same variation trend with respect to the t/d ratio even though a different value of the bolt diameter is considered. This confirms that ρ depends on the t/d ratio and not on the bolt diameter d itself. Additionally, from the simulated set of data it is possible also to observe that, as expected, t/d is directly correlated to the value of the load with a correlation that is practically linear (Fig.15), while e_2/d and e_1/d are inversely correlated to ρ (Figs.16, 17).

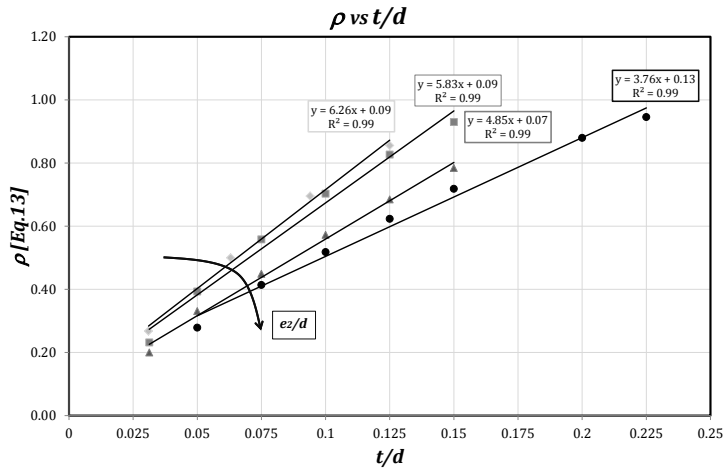

Fig. 15 – Regression curves of the analysed data – dependence of ρ on t/d

From the physical point of view, the influence of the parameter e_2/d on the reduction coefficient ρ is due to the influence that the stiffness of the lateral tube walls have on the value of the elastic buckling load. In fact, as expected, the more the tube walls are close to the hole (lower values of e_2/d), the higher is the buckling critical load.

In order to provide a coefficient to be used in practical design, based on the simulated set of data, a linear multi-parametric regression analysis has been carried out with the aim to find a law providing the value of ρ as a function of t/d, and e_2/d. As verified with former tentative regression models, parameter e_1/d provides a negligible influence on the overall value of ρ and, consequently, can be excluded. Under this assumption, the following equation has been defined, with correlation coefficient equal to 0.85:

$$\rho = 3.36\frac{t}{d} - 0.043\frac{e_2}{d} + 0.39 \tag{16}$$

As a results, combining Eq.(16) and Eq.(15), Eq.(8) proposed by Moze, can be adapted to the case of connections with SHS and long bolts in the following way:

$$\begin{aligned} F_b &= \alpha\alpha_{st} f_u t d \\ \alpha &= min\left(\frac{e_1}{d_0};\ 3\right) \\ \alpha_{st} &= \min\left(3.36\frac{t}{d} - 0.043\frac{e_2}{d} + 0.39;\ 1\right) \end{aligned} \tag{17}$$

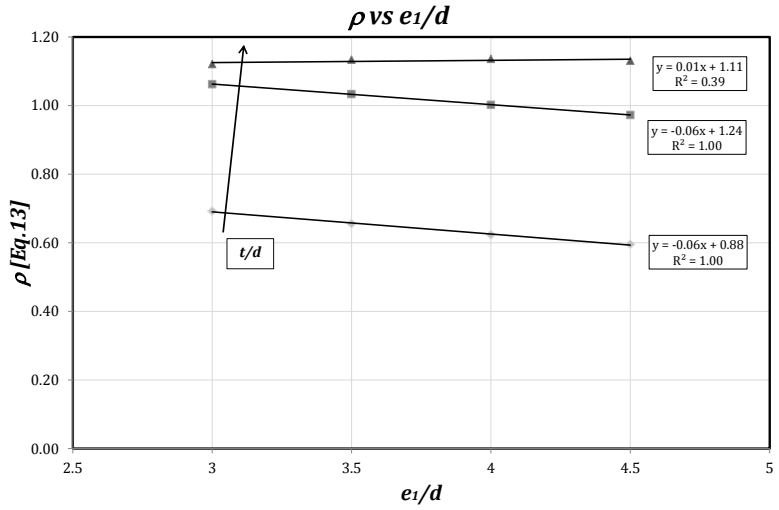

Fig. 16 – Regression curve of the analysed data – dependence of ρ on e_1/d

Finally, by equating Eq.16 to one it is also possible to find the boundary value of t/d separating the buckling and bearing/tear-out failure modes. If t/d of the connection is higher than this limit value, it means that the check for the buckling failure mode can be neglected in practical design:

$$\left(\frac{t}{d}\right)_{limit} = 0.0128\frac{e_2}{d} + 0.181 \tag{18}$$

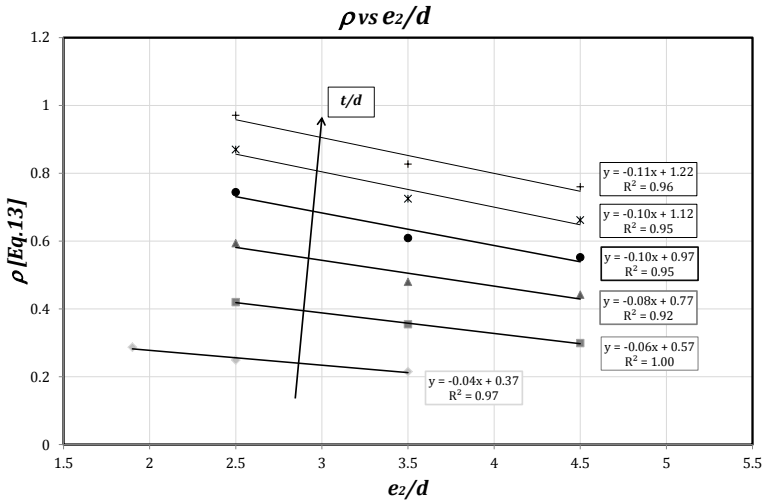

Fig. 17 – Regression curve of the analysed data – dependence of ρ on e_2/d

5. Model validation

The accuracy of the capacity model previously described has been verified by comparison with experimental data and FE results currently available in technical literature. In particular, the reference dataset is composed by the 41 experimental data and FE simulations reported in a recent paper of the same authors [26], which has been extended in this work with further 12 FE simulations, performed running again the same FE model already validated in [26] in order to consider also other cases with a different bolt diameter. Both the experimental and FE results are referred to the same layout, namely that described in Fig.4, which is an elementary connection composed by a SHS tube, fastened with a single long bolt.

The experimental cases of the reference dataset are 24 [26] and regard connections made with SHS tubes of nominal thickness varying from 2 to 4 mm, two different steel grades (S235 and HXLAD420), two different bolt diameters (M12 and M16) and the following range of variation of the main geometrical parameters: $0.1<t/d<0.3$; $2.4<e_1/d<3.5$, $1.9<e_2/d<3.5$. Conversely, the FE simulations, both those carried out in [26] and the additional ones performed in this work, are referred to further 29 cases considering a wider range of variability of the geometries. In particular, the thickness of the tubes considered in the FE simulations varies from 0.50 to 6 mm, while the geometrical parameters vary in the following range: $0.1<t/d<0.4$; $1<e_1/d<5.6$, $0.9<e_2/d<2.5$.

The experimental or simulated values of the ultimate loads, reported in Table 2 (together with a summary of the geometrical and mechanical properties of each one of the analysed cases), have been compared to the values of the load predicted by means of the two models previously set up, expressed by means of Eqs.(16),(17). Additionally, in order to underline the improved accuracy obtained with the proposed models with respect to the codified procedures, the bearing strengths have also been

calculated by means of the formulations proposed by: *i)* AISI S100 (Eqs.1-2), assuming modification factors alternatively equal to 0.75 or 1; *ii)* with the equations proposed by AISC 360-10 for normal lap shear connections (Eq.(3)) or for connections of with long bolts (Eq.(5)); *iii)* with the Eurocode 3 part 1.3 and 1.8 equations (Eqs.(6) and (7)); *iv)* with the model of Može (Eq.(8)). Obviously in all the analysed cases, the strength of the connection (to be compared with the experimental or simulated data) has been determined as minimum between the bearing strength at the bolt's hole and the bolt resistance. The bolt resistance has been calculated according to the EC3 approach as:

$$F_{bolt,EC3} = 0.60 A_b f_{ub} \tag{19}$$

where A_b is the bolt's area which, in the experimental cases, is on one side of the tube the gross area, while on the other side is the net area, and in the cases simulated by means of the FE models it is on both sides the net area, and f_{ub} is the ultimate stress of the bolt material which is considered in all the cases to be 800 MPa.

***Table 2** – Set of Reference Data*

		t/d	e_1/d	e_2/d	e_1/d_0	d [mm]	d_0 [mm]	t [mm]	e_1 [mm]	e_2 [mm]	f_y [MPa]	f_u [MPa]	F_{FEM}-F_{exp} [kN]
Experimental Data [26]	1	0.1	3.1	1.9	3.0	16.0	16.5	2.0	50.3	29.7	398.0	496.0	69.3
	2	0.1	3.0	1.9	2.9	16.0	16.5	2.1	48.7	29.7	398.0	496.0	80.8
	3	0.1	3.1	1.9	3.0	16.0	16.5	2.1	49.0	29.7	398.0	496.0	82.0
	4	0.1	3.1	1.9	3.0	16.0	16.5	2.1	49.1	29.8	398.0	496.0	91.0
	5	0.2	3.3	2.5	3.1	12.0	12.5	2.0	39.3	29.9	398.0	496.0	67.6
	6	0.2	3.3	2.5	3.2	12.0	12.5	2.1	40.0	30.2	398.0	496.0	70.8
	7	0.2	3.3	2.5	3.2	12.0	12.5	2.1	39.9	30.2	398.0	496.0	76.6
	8	0.2	3.3	2.5	3.2	12.0	12.5	2.0	39.9	30.2	398.0	496.0	69.8
	9	0.2	3.3	2.5	3.2	12.0	12.5	2.6	39.6	29.8	434.0	509.0	89.6
	10	0.2	3.3	2.5	3.2	12.0	12.5	2.6	40.0	30.0	434.0	509.0	90.3
	11	0.2	3.5	2.5	3.4	12.0	12.5	2.5	41.9	29.7	434.0	509.0	87.4
	12	0.2	3.4	2.5	3.3	12.0	12.5	2.6	40.8	29.7	434.0	509.0	90.8
	13	0.2	3.1	1.9	3.0	16.0	16.5	2.6	49.6	29.9	434.0	509.0	121.6
	14	0.2	3.2	1.9	3.1	16.0	16.5	2.5	51.7	30.0	434.0	509.0	120.0
	15	0.2	3.2	1.9	3.1	16.0	16.5	2.6	50.9	30.0	434.0	509.0	117.8
	16	0.2	3.1	1.9	3.0	16.0	16.5	2.6	49.5	30.0	434.0	509.0	104.4
	17	0.3	2.8	2.5	2.7	12.0	12.5	3.9	33.2	30.3	401.0	427.0	103.1
	18	0.3	2.8	2.5	2.7	12.0	12.5	3.9	33.4	30.4	401.0	427.0	100.4
	19	0.3	2.8	2.5	2.6	12.0	12.5	3.9	33.1	30.5	401.0	427.0	97.2
	20	0.3	2.8	2.5	2.7	12.0	12.5	3.8	34.1	30.4	401.0	427.0	100.2
	21	0.2	2.6	1.9	2.5	16.0	16.5	3.8	41.5	30.4	401.0	427.0	160.4
	22	0.2	2.4	1.9	2.3	16.0	16.5	3.8	37.6	30.4	401.0	427.0	164.1
	23	0.2	2.5	1.9	2.5	16.0	16.5	3.8	40.6	30.5	401.0	427.0	161.7
	24	0.2	2.6	1.9	2.5	16.0	16.5	3.8	41.3	30.3	401.0	427.0	163.0
FE simulation reported in [26]	25	0.0	3.1	1.9	3.0	16.0	16.5	0.5	50.0	30.0	443.0	499.0	9.7
	26	0.1	3.1	1.9	3.0	16.0	16.5	1.0	50.0	30.0	443.0	499.0	23.8
	27	0.1	3.1	1.9	3.0	16.0	16.5	1.5	50.0	30.0	443.0	499.0	42.8
	28	0.1	3.1	1.9	3.0	16.0	16.5	2.0	50.0	30.0	443.0	499.0	72.9
	29	0.2	3.1	1.9	3.0	16.0	16.5	2.5	50.0	30.0	443.0	499.0	103.9
	30	0.2	3.1	1.9	3.0	16.0	16.5	3.0	50.0	30.0	443.0	499.0	125.6
	31	0.3	3.1	1.9	3.0	16.0	16.5	4.0	50.0	30.0	443.0	499.0	134.4

		t/d	e_1/d	e_2/d	e_1/d_0	d	d_0	t	e_1	e_2	f_y	f_u	F_{FEM}-F_{exp}
	32	0.4	3.1	1.9	3.0	16.0	16.5	6.0	50.0	30.0	443.0	499.0	134.1
	33	0.2	5.6	1.9	5.5	16.0	16.5	2.5	90.0	30.0	443.0	499.0	141.9
	34	0.2	5.0	1.9	4.8	16.0	16.5	2.5	80.0	30.0	443.0	499.0	141.9
	35	0.2	4.4	1.9	4.2	16.0	16.5	2.5	70.0	30.0	443.0	499.0	141.8
	36	0.2	2.5	1.9	2.4	16.0	16.5	2.5	40.0	30.0	443.0	499.0	96.5
	37	0.2	1.9	1.9	1.8	16.0	16.5	2.5	30.0	30.0	443.0	499.0	71.2
	38	0.2	1.6	1.9	1.5	16.0	16.5	2.5	25.0	30.0	443.0	499.0	54.0
	39	0.2	1.0	1.9	1.0	16.0	16.5	2.5	16.5	30.0	443.0	499.0	39.8
	40	0.2	3.1	0.9	3.0	16.0	16.5	2.5	50.0	15.0	443.0	499.0	109.0
	41	0.2	3.1	1.3	3.0	16.0	16.5	2.5	50.0	20.0	443.0	499.0	107.0
New FE Simulations	42	0.0	3.3	2.5	3.2	12.0	12.5	0.5	40.0	30.0	443.0	499.0	8.2
	43	0.1	3.3	2.5	3.2	12.0	12.5	1.0	40.0	30.0	443.0	499.0	20.3
	44	0.1	3.3	2.5	3.2	12.0	12.5	1.5	40.0	30.0	443.0	499.0	35.4
	45	0.2	3.3	2.5	3.2	12.0	12.5	2.0	40.0	30.0	443.0	499.0	67.5
	46	0.2	3.3	2.5	3.2	12.0	12.5	2.5	40.0	30.0	443.0	499.0	80.7
	47	0.3	3.3	2.5	3.2	12.0	12.5	3.0	40.0	30.0	443.0	499.0	84.7
	48	0.3	3.3	2.5	3.2	12.0	12.5	4.0	40.0	30.0	443.0	499.0	84.3
	49	0.2	3.3	1.3	3.2	12.0	12.5	2.5	40.0	15.0	443.0	499.0	80.9
	50	0.2	3.3	1.7	3.2	12.0	12.5	2.5	40.0	20.0	443.0	499.0	82.3
	51	0.1	3.3	1.3	3.2	12.0	12.5	1.5	40.0	15.0	443.0	499.0	40.2
	52	0.1	3.3	1.7	3.2	12.0	12.5	1.5	40.0	20.0	443.0	499.0	38.8
	53	0.1	3.3	2.5	3.2	12.0	12.5	1.5	40.0	30.0	443.0	499.0	37.8

For the sake of shortness, the results of the validation study are summarized in Table 3 reporting for the 8 considered models, the professional factors calculated for each one of the 53 cases, determined as the ratio between the predicted over experimental/simulated value of the maximum load. Additionally, in the same table the min/max and mean values, standard deviation and coefficient of variation of the professional factors obtained with the considered models are reported. Due to the size, the complete table containing the detailed results of the application of the various models is delivered only in a specific annex. The results of the application of the models are also reported in Fig.18, where the experimental or simulated values are graphically compared to the calculated ones.

Table 3 – *Accuracy of the models*

		AISI S100 (Eqs.1,2)		*AISC (Eqs.3,5)*		*EC3*	*Moze*	*Proposal*
		m_f=0.75	m_f=1	Eq.3	Eq.5	Eqs.6,7	Eq.8	Eq.16,17
		PF	PF	PF	PF	PF	PF	PF
Experimental Data [26]	1	1.05	1.40	1.40	0.67	1.17	1.40	1.04
	2	0.93	1.24	1.24	0.60	1.02	1.22	0.92
	3	0.90	1.20	1.20	0.58	0.99	1.19	0.88
	4	0.81	1.08	1.08	0.52	0.90	1.08	0.80
	5	0.80	1.07	1.07	0.52	0.89	1.07	0.91
	6	0.78	1.04	1.04	0.50	0.87	1.04	0.89
	7	0.73	0.97	0.97	0.47	0.81	0.97	0.84
	8	0.78	1.04	1.04	0.50	0.87	1.04	0.89
	9	0.79	1.05	1.05	0.54	0.88	1.05	1.05
	10	0.78	1.04	1.04	0.53	0.86	1.04	1.03
	11	0.79	1.05	1.05	0.54	0.88	1.05	1.04
	12	0.77	1.03	1.03	0.53	0.86	1.03	1.03
	13	0.77	1.03	1.03	0.53	0.86	1.03	0.88

		AISI S100 (Eqs.1,2)		AISC (Eqs.3,5)		EC3	Moze	Proposal
FE simulation reported in [26]	14	0.78	1.03	1.03	0.53	0.86	1.03	0.87
	15	0.81	1.09	1.09	0.56	0.91	1.09	0.93
	16	0.90	1.19	1.19	0.61	0.91	1.19	1.01
	17	0.86	0.92	0.92	0.65	0.85	0.92	0.92
	18	0.89	0.94	0.94	0.67	0.88	0.94	0.94
	19	0.91	0.97	0.97	0.69	0.89	0.97	0.97
	20	0.87	0.95	0.95	0.66	0.88	0.95	0.95
	21	0.73	0.97	0.97	0.55	0.68	0.81	0.81
	22	0.71	0.95	0.87	0.53	0.60	0.72	0.72
	23	0.72	0.96	0.96	0.54	0.66	0.79	0.79
	24	0.72	0.96	0.96	0.54	0.66	0.80	0.80
	25	1.11	1.48	2.47	1.31	1.56	2.47	1.02
	26	1.21	1.61	2.01	1.07	1.54	2.01	1.04
	27	1.23	1.64	1.68	0.89	1.40	1.68	1.05
	28	0.99	1.31	1.31	0.70	1.09	1.31	0.96
	29	0.86	1.15	1.15	0.61	0.96	1.15	0.96
	30	0.86	1.14	1.14	0.61	0.95	1.14	1.07
	31	1.07	1.12	1.12	0.76	1.12	1.12	1.12
	32	1.12	1.12	1.12	1.12	1.12	1.12	1.12
	33	0.63	0.84	0.84	0.45	0.70	0.84	0.70
	34	0.63	0.84	0.84	0.45	0.70	0.84	0.70
	35	0.63	0.84	0.84	0.45	0.70	0.84	0.70
	36	0.93	1.24	1.23	0.66	0.84	1.00	0.84
	37	1.26	1.68	1.14	0.90	0.85	1.02	0.85
	38	1.66	2.22	1.16	1.16	0.93	1.12	0.93
	39	Not applicable to this case					1.00	0.94
	40	0.82	1.10	1.10	0.59	0.92	1.10	0.96
	41	0.84	1.12	1.12	0.60	0.76	1.12	0.96
New FE Simulations	42	0.99	1.31	2.19	1.17	1.39	2.19	0.93
	43	1.24	1.65	1.77	0.94	1.36	1.77	1.00
	44	1.14	1.52	1.52	0.81	1.27	1.52	1.07
	45	0.80	1.06	1.06	0.57	0.89	1.06	0.90
	46	0.83	1.00	1.00	0.59	0.93	1.00	1.00
	47	0.95	0.96	0.96	0.68	0.96	0.96	0.96
	48	0.96	0.96	0.96	0.91	0.96	0.96	0.96
	49	0.83	1.00	1.00	0.59	0.93	1.00	1.00
	50	0.82	0.98	0.98	0.58	0.91	0.98	0.98
	51	1.01	1.34	1.34	0.71	1.12	1.34	1.01
	52	1.04	1.39	1.39	0.74	1.16	1.39	1.03
	53	1.07	1.43	1.4	0.76	1.19	1.43	1.00
Min		*0.63*	*0.84*	*0.84*	*0.45*	*0.60*	*0.72*	*0.70*
Max		*1.66*	*2.22*	*2.47*	*1.31*	*1.56*	*2.47*	*1.12*
Mean Value		***0.92***	***1.16***	***1.17***	***0.67***	***0.96***	***1.15***	***0.94***
st. dev.		***0.19***	***0.26***	***0.33***	***0.20***	***0.21***	***0.34***	***0.10***
CV		***0.21***	***0.23***	***0.28***	***0.30***	***0.22***	***0.29***	***0.11***

The results summarized in Fig.18 and Table 3 show that the proposed model, due to the inclusion of a corrective coefficient able to properly account for the buckling failure mode detected in [26], are able to accurately predict the resistance of the connection. In fact, with the proposed regression (Eq.16),

499 the model provides an accurate estimate of the load, with a professional factor that is on average equal
500 to 0.94, with a very low coefficient of variation, equal to the 11%. As expected, due to the assumption
501 related to the maximum achievable bearing strength which, following the suggestion made by Moze
502 [3] has been limited to 3, the model results to be slightly conservative. Conversely, as already
503 preliminarily pointed out in [26], the codified models do not seem to provide a sufficient accuracy and,
504 in fact, even though some of them (e.g. EC3 and AISI S100 with modification factor equal to 0.75) can
505 achieve mean values of the professional factors close to one, they are not able to accurately predict the
506 resistance in many cases. This is demonstrated by the high dispersion of the professional factors
507 (ranging from 0.6 to 1.6 for EC3 and AISI S100) and high coefficients of variation (21% and 22% for
508 AISI S100 and EC3). As expected, the model of Može, (Eq.8) and the model suggested by AISC 360-10
509 (Eq.(3)), being developed for overlapped connections with a full out-of-plane confinement of the bolt's
510 hole, overestimate significantly the value of the ultimate capacity and provide high values of the
511 coefficient of variation, (28% and 29% for AISC and Može models). Additionally, as also expected, the
512 model suggested by AISC 360-10 for connections with long bolts (Eq.5) significantly underestimates
513 the resistance because it represents mainly a conservative extension of the formula normally used for
514 pins in bearing. Indeed in case of application of Eq.(5) the mean value of the professional factor results
515 to be equal to 0.67 with a coefficient of variation equal to the 30%.

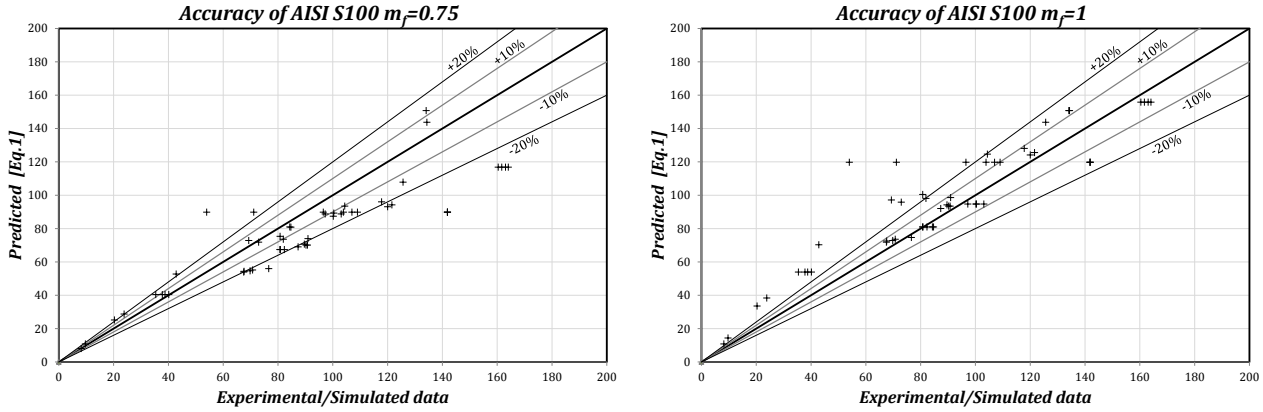

516

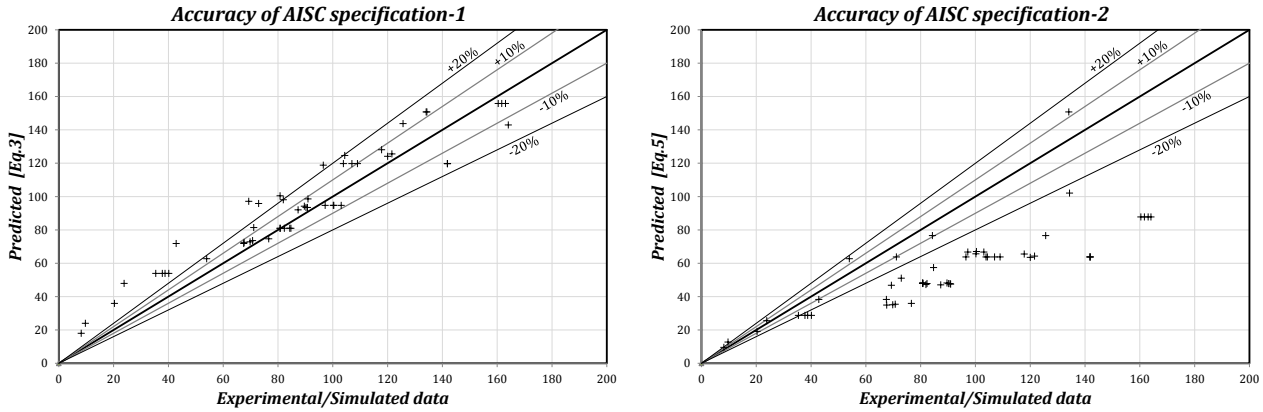

517

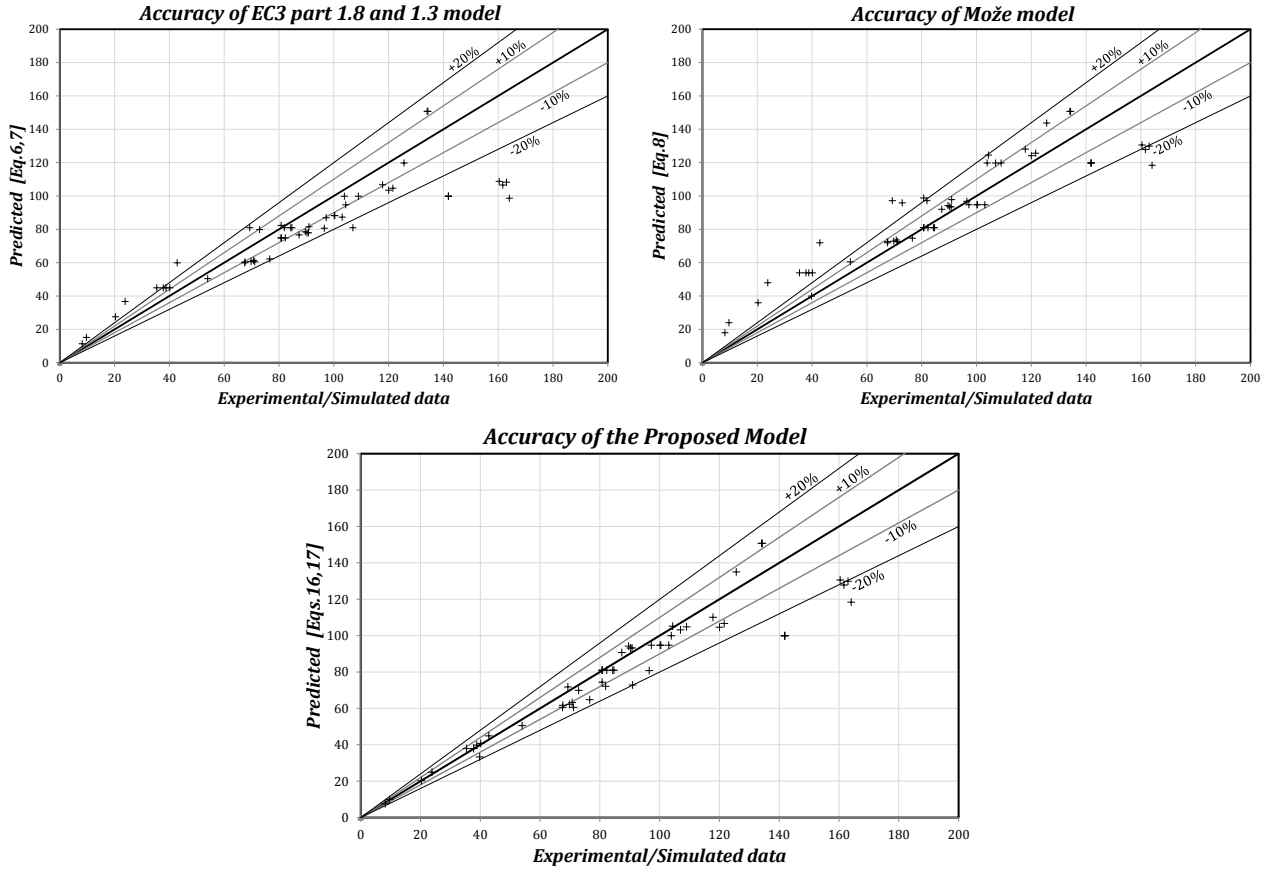

Fig. 18 – Accuracy of the models (literature and proposed)

6. Conclusions

In this work the behaviour of connections made with SHS and long bolts has been investigated. The work developed has been mainly motivated by the preliminary results obtained in a previous experimental analysis developed at the Laboratory on Materials and Structures of the University of Liège. The previous work has evidenced a particular buckling failure mode which is not explicitly considered neither in the current EC3 formulas nor in other codified design procedures or literature models, such as AISI S100, AISC 360-10 or the model recently proposed by Može in view of the definition of a new Eurocode standard. In fact, such experimental analysis pointed out that in case of connections made with tubular members and long bolts, the lack of confinement effect in the internal part of the tube may lead during the load process to the development of a particular type of out-of-plane local buckling of the bolt hole (Fig.6). Therefore, due to this experimental observation, the analyses performed in this paper have been devoted to the development of a design equation for this particular connection's typology, based on the recent proposal of Može, able to account for the possible development of local buckling at the bolt hole.

In order to define a design formula, a procedure able to predict the ultimate load of the tube's plate subjected to the action applied from the bolt in bearing has been set up. This procedure has been

based on the application of the Winter's approach for the determination of the post-elastic buckling load and on the development of a simplified FE model in SAP 2000 to determine the elastic buckling load. Afterwards, exploiting the developed approach, a parametric analysis has been carried out in order to define a correlation between the reduction of resistance due to the buckling failure mode and the geometrical properties of the tube plate. The analysis has shown that the local buckling effects, in the analysed connection, may be significant depending on the values of t/d, e_1/d and of e_2/d demonstrating that the buckling check is necessary if t/d is lower than the limit values given by Eqs. (19) and (20). Finally, in order to define a simple coefficient to be used in design to account for this particular failure mode, a regression analysis of the data generated by means of parametric simulations has been carried out, proposing to calculate the bearing resistance at bolt hole in case of connections made with SHS and long bolts adopting one of the two models described in Eq.(18).

The proposed design equations have been validated against a reference dataset of 53 tests or FE simulations, in part collected from [26] and in part developed within this work. The comparison between the data and the predictions obtained with the proposed equation and with other six literature models has evidenced the poor accuracy of the classical bearing models (calibrated mainly on lap shear connections) for this specific type of connection, as well as the improved accuracy obtained with the proposed model which is able to achieve a mean professional factor equal to 0.94, with a coefficient of variation lower than the 11%.

REFERENCES

[1] Može, P. and Beg, D., 2011. "Investigation of high strength steel connections with several bolts in double shear". Journal of Constructional Steel Research, 67(3), 333-347.

[2] Može, P. and Beg, D., 2014. "A complete study of bearing stress in single bolt connections". Journal of Constructional Steel Research, 95, 126-140.

[3] Može, P., 2016. "On the bearing resistance of bolted connections". Eighth International Workshop on Connections in Steel Structures 2016, Boston.

[4] CEN, 2005. Eurocode 3: Design of steel structures - Part 1-8: Design of joints. European Committee for Standardization, CEN, Brussels.

[5] CEN, 2005. Eurocode 3: Design of steel structures - Part 1-3: General rules. Supplementary rules for col-formed members and sheeting. European Committee for Standardization, CEN, Brussels

[6] American Iron and Steel Institute, AISI S100, 2016. "North American Specification for the Design of Cold-Formed Steel Structural Members ", Canadian Standards Association.

[7] AISC 360-10 (2010). Specification for structural steel buildings. Chicago: American Institute of steel construction.

[8] H. Draganić, T. Dokšanović, D. Markulak,(2014). Investigation of bearing failure in steel single bolt lap connections, Journal of Constructional Steel Research, Volume 98, Pages 59-72

[9] L. Teh, M. Uz (2015). Ultimate shear-out capacities of structural –steel bolted connections, Journal of Structural Engineering, ASCE, Volume 141 (6)
[10] AISC (1993). Load and resistance factor design specification for structural steel buildings. Chicago: American Institute of steel construction.
[11] Salih E.L., Gardner L. and Nethercot D.A., 2011. "Bearing failure in stainless steel bolted connections", Engineering Structures, Vol 33, 549-562.
[12] Kim TS, Kuwamura H., 2007. "Finite element modelling of bolted connections in thin-walled stainless steel plates under static shear". Thin-walled Structures, Vol.45(4), 407-21.
[13] Kiymaz G., 2009, "Bearing strength of stainless steel bolted plates in tension", Nordic Steel Construction Conference, Marmo, 2-4 September.
[14] L. Teh, M. Uz (2017). "Ultimate Tilt-Bearing Capacity of Bolted Connections in Cold-Reduced Steel Sheets", Journal of Structural Engineering, ASCE, Volume 143 (4)
[15] Teh, L. H., and Clements, D. D. A. (2012). "Block shear capacity of bolted connections in cold-reduced steel sheets." J. Struct. Eng., 10.1061/(ASCE)ST.1943-541X.0000478, 459–467.
[16] Teh, L. H., and Gilbert, B. P. (2012). "Net section tension capacity of bolted connections in cold-reduced steel sheets." J. Struct. Eng., 10.1061/(ASCE)ST.1943-541X.0000477, 337–344.
[17] Teh, L. H., and Uz, M. E. (2014). "Effect of loading direction on the bearing capacity of cold-reduced sheet steels." J. Struct. Eng., 10.1061/(ASCE) ST.1943-541X.0001107, 06014005.
[18] Puthli R., Fleischer O., 2001. "Investigations on bolted connections for high strength steel members", Journal of Constructional Steel research 57 (2001), 313-326.
[19] Kim, H. J., and Yura, J. A. (1999) "The effect of ultimate-to-yield ratio on the bearing strength of bolted connections." J. Construct. Steel Res., 49, 255-269
[20] Aalberg, A. and Larsen, P. K. (2001) "Bearing strength of bolted connections in high strength steel." Proc. 9th 427 Nordic Steel Construction Conf., Helsinki, Finland, 859–866.
[21] Rex, C. O. and Easterling, W. S. (2003) "Behavior and modelling of a bolt bearing on a single plate." J. Struct. Eng., 129 (6), 792–800.
[22] Kouhi, J. and Kortesmaa, M. (1990) Strength tests on bolted connections using high-strength steels (HSS steels) as a base material, Espoo:Technical Research Centre of Finland.
[23] Može, P. and Beg, D. (2010) 'High strength steel tension splices with one or two bolts', Journal of Constructional Steel Research, 66(8-9), 1000-1010.
[24] Chung KF, Lau L. (1999) "*Experimental investigation on bolted moment connections among cold formed steel members*". Engineering Structures 1999;21(10): 898_911.
[25] C Yu, MX Panyanouvong, "Bearing strength of cold-formed steel bolted connections with a gap" Thin-Walled Structures, Volume 67, June 2013, Pages 110-115
[26] D'Antimo M., Demonceau JF, Jaspart JP, Latour M, Rizzano G (2017), "Experimental and theoretical analysis of shear bolted connections for tubular racking structures", Accepted with major revisions on Journal of Constructional Steel Research.
[27] Winter G. (1947), "Strength of thin steel compression flanges". Reprint No. 32. Ithaca, NY, USA: Cornell University Engineering Experimental Station.
[28] CSI (2015). SAP2000 v.16.0.1 – Analysis Reference Manual.
[29] Yu WW. (1982). AISI design criteria for bolted connections. In: Proceedings of the sixth international specialty conference on cold-formed steel structure, University of Missouri-Rolla.
[30] Zadanferrokh F, Bryan ER. (1992). Testing and design of bolted connections in cold-formed steel sections. In: Proceedings of 11th international specialty conference on cold-formed steel structures, St. Louis, Missouri.

[31] LaBoube RA, Yu WW. (1995). Tensile and bearing capacities of bolted connections. Final Summary Report, Civil Engineering Study 95-96, ColdFormed

[32] Wallace JA, Schuster RM, LaBoube R. (2001a). Testing of bolted cold-formed steel connections in bearing (with and without washers), Report RP01-4, American Iron and Steel Institute, Washington, DC.

[33] Wallace JA, Schuster RM, LaBoube R. (2001b). Calibrations of bolted coldformed steel connections in bearing (with and without washers), Report RP01-5, American Iron and Steel Institute, Washington, DC.

[34] Rogers, C.A and G.J. Hancock (1998), "New Bolted Connection Design Formulae for G550 and G300 Steels less than 1.0 mm Thick," Research Report No. R769, Centre for Advanced Structural Engineering, Department of Civil Engineering, University of Sydney, Sidney, Australia, June 1998.

[35] Rogers, C.A and G.J. Hancock (1999), "Bolted Connection Design for Sheet Steels less than 1.0 mm Thick," Journal of Constructional Steel Research, Vol. 51. No.2, 123-146.

[36] Rogers CA, Hancock GJ. Ductility of G550 sheet steels in tension—elongation measurements and perforated tests. Research Report No. R735, Centre for Advanced Structural Engineering, University of Sydney, Sydney, NSW, Australia, 1996.

[37] Rogers CA, Hancock GJ. Ductility of G550 sheet steels subjected to tension. Proceedings of the 5th International Colloquium on Stability and Ductility of Steel Structures, Japanese Society of Steel Construction and Nagoya University, Nagoya, Japan, 1997:949–956.

[38] Rogers CA, Hancock GJ. Ductility of G550 sheet steels in tension. Journal of Structural Engineering ASCE 1997;123(12):1586–94.

[39] Rogers CA, Hancock GJ. Bolted connection tests of thin G550 and G300 sheet steels. Research Report No. R749, Centre for Advanced Structural Engineering, University of Sydney, Sydney, NSW, Australia, 1997.

[40] Rogers CA, Hancock GJ. Bolted connection tests of thin G550 and G300 sheet steels. Journal of Structural Engineering, ASCE 1998;124(7):798–808.

[41] Rogers CA, Hancock GJ. New bolted connection design formulae for G550 and G300 sheet steels less than 1.0 mm thick. Research Report No. R769, Centre for Advanced Structural Engineering, University of Sydney, Sydney, NSW, Australia, 1998.

[42] AS/NZS 4600:2005. (2005). Cold-formed steel structures. Joint Technical Committee BD-082.

[43] Snijder H. H., Ungerman D., Stark J.W.B., Sedlacek G., Bijlaard F.S.K., HemmertHalswick A.: Evaluation of test results on welded connections in order to obtain strength functions and suitable model factors, Part A Results, Background documentation, 6.05, BI 88-139, Delft 1988.

[44] Snijder H. H., Ungerman D., Stark J.W.B., Sedlacek G., Bijlaard F.S.K., HemmertHalswick A.: Evaluation of test results on welded connections in order to obtain strength functions and suitable model factors, Part B: Evaluation , Background documentation, 6.06, BI-88-139, Delft 1988.

[45] Snijder, H. H., Ungermann, D., Stark, J. W. B., Sedlacek, G., Bijlaard, F. S. K. and Hemmert-Halswick, A. (1988) Evaluation of test results on bolted connections in order to obtain strength functions and suitable model factors - Part C: Test data, Brussels:Commission of the European Communities.

[46] Kirchhoff G (1950). Über das Gleichgewicht and die Bewegung einer elastischen Scheibe, Journal für reine und angewandte Mathematik, 40: 51-88

662 [47] Von Karman T. (1910), “Festigheitsprobleme im Maschinenbau”. Encyclopaedie der
663 Mathematischen Wissenschaften.

ANNEX – DETAILED CALCULATIONS OF THE BEARING STRENGTH WITH THE MODELS REPORTED IN TABLE 3

Accuracy of AISI S100 models

	F_{FEM}-F_{exp} [kN]	$F_{bolt,EC3}$ [kN]	$C_{AISI\ S100}$ Eq.(2)	$F_{b,AISI\ S100}$ m_f=0.75 Eq.(1)/[kN]	min[$F_{b,mf=0.75}$;$F_{bolt,EC3}$] [kN]	ratio	$F_{b,AISI\ S100}$ m_f=1 Eq.(1)/[kN]	min[$F_{b,mf=1}$;$F_{bolt,EC3}$] [kN]	ratio
1	69.3	171.8	3.0	72.9	72.9	1.05	97.1	97.1	1.40
2	80.8	171.8	3.0	75.4	75.4	0.93	100.5	100.5	1.24
3	82.0	171.8	3.0	73.6	73.6	0.90	98.1	98.1	1.20
4	91.0	171.8	3.0	73.9	73.9	0.81	98.6	98.6	1.08
5	67.6	94.7	3.0	54.4	54.4	0.80	72.5	72.5	1.07
6	70.8	94.7	3.0	55.2	55.2	0.78	73.6	73.6	1.04
7	76.6	94.7	3.0	56.0	56.0	0.73	74.6	74.6	0.97
8	69.8	94.7	3.0	54.6	54.6	0.78	72.9	72.9	1.04
9	89.6	94.7	3.0	70.6	70.6	0.79	94.2	94.2	1.05
10	90.3	94.7	3.0	70.1	70.1	0.78	93.5	93.5	1.04
11	87.4	94.7	3.0	69.0	69.0	0.79	92.0	92.0	1.05
12	90.8	94.7	3.0	70.1	70.1	0.77	93.5	93.5	1.03
13	121.6	171.8	3.0	94.2	94.2	0.77	125.6	125.6	1.03
14	120.0	171.8	3.0	93.1	93.1	0.78	124.1	124.1	1.03
15	117.8	171.8	3.0	96.0	96.0	0.81	128.0	128.0	1.09
16	104.4	171.8	3.0	93.5	93.5	0.90	124.6	124.6	1.19
17	103.1	94.7	3.0	88.8	88.8	0.86	118.4	94.7	0.92
18	100.4	94.7	3.0	89.2	89.2	0.89	119.0	94.7	0.94
19	97.2	94.7	3.0	88.8	88.8	0.91	118.4	94.7	0.97
20	100.2	94.7	3.0	87.4	87.4	0.87	116.5	94.7	0.95
21	160.4	171.8	3.0	116.8	116.8	0.73	155.8	155.8	0.97
22	164.1	171.8	3.0	116.8	116.8	0.71	155.8	155.8	0.95
23	161.7	171.8	3.0	116.8	116.8	0.72	155.8	155.8	0.96
24	163.0	171.8	3.0	116.8	116.8	0.72	155.8	155.8	0.96
25	9.7	150.7	1.8	10.8	10.8	1.11	14.4	14.4	1.48
26	23.8	150.7	2.4	28.7	28.7	1.21	38.3	38.3	1.61
27	42.8	150.7	2.9	52.7	52.7	1.23	70.3	70.3	1.64

	F_{FEM}-F_{exp}	$F_{bolt,EC3}$	$C_{AISI\ S100}$	$F_{b,AISI\ S100}$ m_f=0.75	$min[F_{b,mf=0.75};F_{bolt,EC3}]$	ratio	$F_{b,AISI\ S100}$ m_f=1	$min[F_{b,mf=1};F_{bolt,EC3}]$	ratio
28	72.9	150.7	3.0	71.9	71.9	0.99	95.8	95.8	1.31
29	103.9	150.7	3.0	89.8	89.8	0.86	119.8	119.8	1.15
30	125.6	150.7	3.0	107.8	107.8	0.86	143.7	143.7	1.14
31	134.4	150.7	3.0	143.7	143.7	1.07	191.6	150.7	1.12
32	134.1	150.7	3.0	215.6	150.7	1.12	287.4	150.7	1.12
33	141.9	150.7	3.0	89.8	89.8	0.63	119.8	119.8	0.84
34	141.9	150.7	3.0	89.8	89.8	0.63	119.8	119.8	0.84
35	141.8	150.7	3.0	89.8	89.8	0.63	119.8	119.8	0.84
36	96.5	150.7	3.0	89.8	89.8	0.93	119.8	119.8	1.24
37	71.2	150.7	3.0	89.8	89.8	1.26	119.8	119.8	1.68
38	54.0	150.7	3.0	89.8	89.8	1.66	119.8	119.8	2.22
39	39.8	150.7	CODE PROVISIONS NOT APPLICABLE TO THIS CASE						
40	109.0	150.7	3.0	89.8	89.8	0.82	119.8	119.8	1.10
41	107.0	150.7	3.0	89.8	89.8	0.84	119.8	119.8	1.12
42	8.2	80.9	1.8	8.1	8.1	0.99	10.8	10.8	1.31
43	20.3	80.9	2.8	25.1	25.1	1.24	33.5	33.5	1.65
44	35.4	80.9	3.0	40.4	40.4	1.14	53.9	53.9	1.52
45	67.5	80.9	3.0	53.9	53.9	0.80	71.9	71.9	1.06
46	80.7	80.9	3.0	67.4	67.4	0.83	89.8	80.9	1.00
47	84.7	80.9	3.0	80.8	80.8	0.95	107.8	80.9	0.96
48	84.3	80.9	3.0	107.8	80.9	0.96	143.7	80.9	0.96
49	80.9	80.9	3.0	67.4	67.4	0.83	89.8	80.9	1.00
50	82.3	80.9	3.0	67.4	67.4	0.82	89.8	80.9	0.98
51	40.2	80.9	3.0	40.4	40.4	1.01	53.9	53.9	1.34
52	38.8	80.9	3.0	40.4	40.4	1.04	53.9	53.9	1.39
53	37.8	80.9	3.0	40.4	40.4	1.07	53.9	53.9	1.43
					Min	0.63		***Min***	0.84
					Max	1.66		***Max***	2.22
					Mean Value	***0.92***		***Mean Value***	***1.16***
					Standard Deviation	***0.19***		***Standard Deviation***	***0.26***
					Coefficient of Variation	***0.21***		***Coefficient of Variation***	***0.23***

668 ***Accuracy of AISC models***

	F_{FEM}-F_{exp} [kN]	$F_{bolt,EC3}$ [kN]	$F_{b,AISC}$ Eq.(3)	$min[F_{b,AISC};F_{bolt,EC3}]$ [kN]	ratio	$F_{b,AISC}$ Eq.(5)	$min[F_{b,AISC};F_{bolt,EC3}]$ [kN]	ratio
1	69.3	171.8	97.1	97.1	1.40	46.8	46.8	0.67
2	80.8	171.8	100.5	100.5	1.24	48.4	48.4	0.60
3	82.0	171.8	98.1	98.1	1.20	47.2	47.2	0.58
4	91.0	171.8	98.6	98.6	1.08	47.5	47.5	0.52
5	67.6	94.7	72.5	72.5	1.07	34.9	34.9	0.52
6	70.8	94.7	73.6	73.6	1.04	35.4	35.4	0.50
7	76.6	94.7	74.6	74.6	0.97	35.9	35.9	0.47
8	69.8	94.7	72.9	72.9	1.04	35.1	35.1	0.50
9	89.6	94.7	94.2	94.2	1.05	48.2	48.2	0.54
10	90.3	94.7	93.5	93.5	1.04	47.8	47.8	0.53
11	87.4	94.7	92.0	92.0	1.05	47.1	47.1	0.54
12	90.8	94.7	93.5	93.5	1.03	47.8	47.8	0.53
13	121.6	171.8	125.6	125.6	1.03	64.2	64.2	0.53
14	120.0	171.8	124.1	124.1	1.03	63.5	63.5	0.53
15	117.8	171.8	128.0	128.0	1.09	65.5	65.5	0.56
16	104.4	171.8	124.6	124.6	1.19	63.7	63.7	0.61
17	103.1	94.7	118.4	94.7	0.92	66.7	66.7	0.65
18	100.4	94.7	119.0	94.7	0.94	67.0	67.0	0.67
19	97.2	94.7	118.4	94.7	0.97	66.7	66.7	0.69
20	100.2	94.7	116.5	94.7	0.95	65.7	65.7	0.66
21	160.4	171.8	155.8	155.8	0.97	87.8	87.8	0.55
22	164.1	171.8	142.9	142.9	0.87	87.8	87.8	0.53
23	161.7	171.8	155.8	155.8	0.96	87.8	87.8	0.54
24	163.0	171.8	155.8	155.8	0.96	87.8	87.8	0.54
25	9.7	150.7	24.0	24.0	2.47	12.8	12.8	1.31
26	23.8	150.7	47.9	47.9	2.01	25.5	25.5	1.07
27	42.8	150.7	71.9	71.9	1.68	38.3	38.3	0.89
28	72.9	150.7	95.8	95.8	1.31	51.0	51.0	0.70
29	103.9	150.7	119.8	119.8	1.15	63.8	63.8	0.61
30	125.6	150.7	143.7	143.7	1.14	76.6	76.6	0.61

	F_{FEM}-F_{exp}	$F_{bolt,EC3}$	$F_{b,AISC}$	$min[F_{b,AISC};F_{bolt,EC3}]$	ratio	$F_{b,AISC}$	$min[F_{b,AISC};F_{bolt,EC3}]$	ratio
31	134.4	150.7	191.6	150.7	1.12	102.1	102.1	0.76
32	134.1	150.7	287.4	150.7	1.12	153.1	150.7	1.12
33	141.9	150.7	119.8	119.8	0.84	63.8	63.8	0.45
34	141.9	150.7	119.8	119.8	0.84	63.8	63.8	0.45
35	141.8	150.7	119.8	119.8	0.84	63.8	63.8	0.45
36	96.5	150.7	118.8	118.8	1.23	63.8	63.8	0.66
37	71.2	150.7	81.4	81.4	1.14	63.8	63.8	0.90
38	54.0	150.7	62.7	62.7	1.16	62.7	62.7	1.16
39	39.8	150.7	CODE PROVISIONS NOT APPLICABLE TO THIS CASE					
40	109.0	150.7	119.8	119.8	1.10	63.8	63.8	0.59
41	107.0	150.7	119.8	119.8	1.12	63.8	63.8	0.60
42	8.2	80.9	18.0	18.0	2.19	9.6	9.6	1.17
43	20.3	80.9	35.9	35.9	1.77	19.1	19.1	0.94
44	35.4	80.9	53.9	53.9	1.52	28.7	28.7	0.81
45	67.5	80.9	71.9	71.9	1.06	38.3	38.3	0.57
46	80.7	80.9	89.8	80.9	1.00	47.8	47.8	0.59
47	84.7	80.9	107.8	80.9	0.96	57.4	57.4	0.68
48	84.3	80.9	143.7	80.9	0.96	76.6	76.6	0.91
49	80.9	80.9	89.8	80.9	1.00	47.8	47.8	0.59
50	82.3	80.9	89.8	80.9	0.98	47.8	47.8	0.58
51	40.2	80.9	53.9	53.9	1.34	28.7	28.7	0.71
52	38.8	80.9	53.9	53.9	1.39	28.7	28.7	0.74
53	37.8	80.9	53.9	53.9	1.4	28.7	28.7	0.76
				Min	0.84		***Min***	0.45
				Max	2.47		***Max***	1.31
				Mean Value	***1.17***		***Mean Value***	***0.67***
				Standard Deviation	***0.33***		***Standard Deviation***	***0.20***
				Coefficient of Variation	***0.28***		***Coefficient of Variation***	***0.30***

669

670

671 ***Accuracy of EC3 part 1.3 and part 1.8 model and Moze model***

	F_{FEM}-F_{exp} [kN]	$F_{bolt,EC3}$ [kN]	$k\alpha$ Eqs.(6,7)	$F_{b,EC3}$ Eq.(6,7)	$min[F_{b,EC3};F_{bolt,EC3}]$ [kN]	ratio	α Eq.(8)	$F_{b,Moze}$ Eq.(8)	$min[F_{b,Moze};F_{bolt,EC3}]$ [kN]	ratio
1	69.3	171.8	2.5	80.9	80.9	1.17	3.0	97.1	97.1	1.40
2	80.8	171.8	2.5	82.3	82.3	1.02	2.9	98.8	98.8	1.22
3	82.0	171.8	2.5	80.9	80.9	0.99	3.0	97.1	97.1	1.19
4	91.0	171.8	2.5	81.5	81.5	0.90	3.0	97.8	97.8	1.08
5	67.6	94.7	2.5	60.4	60.4	0.89	3.0	72.5	72.5	1.07
6	70.8	94.7	2.5	61.3	61.3	0.87	3.0	73.6	73.6	1.04
7	76.6	94.7	2.5	62.2	62.2	0.81	3.0	74.6	74.6	0.97
8	69.8	94.7	2.5	60.7	60.7	0.87	3.0	72.9	72.9	1.04
9	89.6	94.7	2.5	78.5	78.5	0.88	3.0	94.2	94.2	1.05
10	90.3	94.7	2.5	77.9	77.9	0.86	3.0	93.5	93.5	1.04
11	87.4	94.7	2.5	76.7	76.7	0.88	3.0	92.0	92.0	1.05
12	90.8	94.7	2.5	77.9	77.9	0.86	3.0	93.5	93.5	1.03
13	121.6	171.8	2.5	104.7	104.7	0.86	3.0	125.6	125.6	1.03
14	120.0	171.8	2.5	103.4	103.4	0.86	3.0	124.1	124.1	1.03
15	117.8	171.8	2.5	106.7	106.7	0.91	3.0	128.0	128.0	1.09
16	104.4	171.8	2.5	103.7	94.7	0.91	3.0	124.5	124.5	1.19
17	103.1	94.7	2.2	87.2	87.2	0.85	2.7	104.7	94.7	0.92
18	100.4	94.7	2.2	88.2	88.2	0.88	2.7	105.8	94.7	0.94
19	97.2	94.7	2.2	86.9	86.9	0.89	2.6	104.3	94.7	0.97
20	100.2	94.7	2.3	88.2	88.2	0.88	2.7	105.9	94.7	0.95
21	160.4	171.8	2.1	108.8	108.8	0.68	2.5	130.5	130.5	0.81
22	164.1	171.8	1.9	98.6	98.6	0.60	2.3	118.4	118.4	0.72
23	161.7	171.8	2.1	106.5	106.5	0.66	2.5	127.8	127.8	0.79
24	163.0	171.8	2.1	108.2	108.2	0.66	2.5	129.9	129.9	0.80
25	9.7	150.7	1.9	15.2	15.2	1.56	3.0	24.0	24.0	2.47
26	23.8	150.7	2.3	36.7	36.7	1.54	3.0	47.9	47.9	2.01
27	42.8	150.7	2.5	59.9	59.9	1.40	3.0	71.9	71.9	1.68
28	72.9	150.7	2.5	79.8	79.8	1.09	3.0	95.8	95.8	1.31
29	103.9	150.7	2.5	99.8	99.8	0.96	3.0	119.8	119.8	1.15
30	125.6	150.7	2.5	119.8	119.8	0.95	3.0	143.7	143.7	1.14

	F_{FEM}-F_{exp}	$F_{bolt,EC3}$	$k\alpha$	$F_{b,EC3}$	$min[F_{b,EC3};F_{bolt,EC3}]$	ratio	α	$F_{b,Moze}$	$min[F_{b,Moze};F_{bolt,EC3}]$	ratio
31	134.4	150.7	2.5	159.7	150.7	1.12	3.0	191.6	150.7	1.12
32	134.1	150.7	2.5	239.5	150.7	1.12	3.0	287.4	150.7	1.12
33	141.9	150.7	2.5	99.8	99.8	0.70	3.0	119.8	119.8	0.84
34	141.9	150.7	2.5	99.8	99.8	0.70	3.0	119.8	119.8	0.84
35	141.8	150.7	2.5	99.8	99.8	0.70	3.0	119.8	119.8	0.84
36	96.5	150.7	2.0	80.6	80.6	0.84	2.4	96.8	96.8	1.00
37	71.2	150.7	1.5	60.5	60.5	0.85	1.8	72.6	72.6	1.02
38	54.0	150.7	1.3	50.4	50.4	0.93	1.5	60.5	60.5	1.12
39	39.8	150.7	CODE PROVISIONS NOT APPLICABLE TO THIS CASE				1.0	39.9	39.9	1.0
40	109.0	150.7	2.5	99.8	99.8	0.92	3.0	119.8	119.8	1.10
41	107.0	150.7	2.5	99.8	80.9	0.76	3.0	119.8	119.8	1.12
42	8.2	80.9	1.9	11.4	11.4	1.39	3.0	18.0	18.0	2.19
43	20.3	80.9	2.3	27.5	27.5	1.36	3.0	35.9	35.9	1.77
44	35.4	80.9	2.5	44.9	44.9	1.27	3.0	53.9	53.9	1.52
45	67.5	80.9	2.5	59.9	59.9	0.89	3.0	71.9	71.9	1.06
46	80.7	80.9	2.5	74.9	74.9	0.93	3.0	89.8	80.9	1.00
47	84.7	80.9	2.5	89.8	80.9	0.96	3.0	107.8	80.9	0.96
48	84.3	80.9	2.5	119.8	80.9	0.96	3.0	143.7	80.9	0.96
49	80.9	80.9	2.5	74.9	74.9	0.93	3.0	89.8	80.9	1.00
50	82.3	80.9	2.5	74.9	74.9	0.91	3.0	89.8	80.9	0.98
51	40.2	80.9	2.5	44.9	44.9	1.12	3.0	53.9	53.9	1.34
52	38.8	80.9	2.5	44.9	44.9	1.16	3.0	53.9	53.9	1.39
53	37.8	80.9	2.5	44.9	44.9	1.19	3.0	53.9	53.9	1.43
					Min	0.60			***Min***	0.72
					Max	1.56			***Max***	2.47
					Mean Value	***0.96***			***Mean Value***	***1.15***
					Standard Deviation	***0.21***			***Standard Deviation***	***0.34***
					Coefficient of Variation	***0.22***			***Coefficient of Variation***	***0.29***

672

673

Accuracy of the proposed model

	F_{FEM}-F_{exp} [kN]	$F_{bolt,EC3}$ [kN]	α_{st} Eq.(16)	$F_{b,Proposal}$ Eq.(17)	$min[F_{b,Proposal};F_{bolt,EC3}]$ [kN]	ratio
1	69.3	171.8	0.74	71.8	71.8	1.04
2	80.8	171.8	0.75	74.4	74.4	0.92
3	82.0	171.8	0.74	72.1	72.1	0.88
4	91.0	171.8	0.74	72.8	72.8	0.80
5	67.6	94.7	0.85	61.7	61.7	0.91
6	70.8	94.7	0.86	63.2	63.2	0.89
7	76.6	94.7	0.87	64.7	64.7	0.84
8	69.8	94.7	0.85	62.2	62.2	0.89
9	89.6	94.7	1.00	94.2	94.2	1.05
10	90.3	94.7	1.00	93.1	93.1	1.03
11	87.4	94.7	0.99	90.7	90.7	1.04
12	90.8	94.7	1.00	93.2	93.2	1.03
13	121.6	171.8	0.85	106.7	106.7	0.88
14	120.0	171.8	0.84	104.6	104.6	0.87
15	117.8	171.8	0.86	110.0	110.0	0.93
16	104.4	171.8	0.84	105.2	105.2	1.01
17	103.1	94.7	1.00	104.7	94.7	0.92
18	100.4	94.7	1.00	105.8	94.7	0.94
19	97.2	94.7	1.00	104.3	94.7	0.97
20	100.2	94.7	1.00	105.9	94.7	0.95
21	160.4	171.8	1.00	130.5	130.5	0.81
22	164.1	171.8	1.00	118.4	118.4	0.72
23	161.7	171.8	1.00	127.8	127.8	0.79
24	163.0	171.8	1.00	129.9	129.9	0.80
25	9.7	150.7	0.41	9.9	9.9	1.02
26	23.8	150.7	0.52	24.9	24.9	1.04
27	42.8	150.7	0.62	44.9	44.9	1.05
28	72.9	150.7	0.73	69.9	69.9	0.96
29	103.9	150.7	0.83	99.9	99.9	0.96
30	125.6	150.7	0.94	135.0	135.0	1.07
31	134.4	150.7	1.00	191.6	150.7	1.12
32	134.1	150.7	1.00	287.4	150.7	1.12
33	141.9	150.7	0.83	99.9	99.9	0.70
34	141.9	150.7	0.83	99.9	99.9	0.70
35	141.8	150.7	0.83	99.9	99.9	0.70
36	96.5	150.7	0.83	80.7	80.7	0.84
37	71.2	150.7	0.83	60.6	60.6	0.85

	F_{FEM}-F_{exp}	$F_{bolt,EC3}$	α_{st}	$F_{b,Proposal}$	$min[F_{b,Proposal};F_{bolt,EC3}]$	ratio
38	54.0	150.7	0.83	50.5	50.5	0.93
39	39.8	150.7	0.83	33.3	33.3	0.84
40	109.0	150.7	0.87	104.8	104.8	0.96
41	107.0	150.7	0.86	103.1	103.1	0.96
42	8.2	80.9	0.42	7.6	7.6	0.93
43	20.3	80.9	0.56	20.2	20.2	1.00
44	35.4	80.9	0.70	37.9	37.9	1.07
45	67.5	80.9	0.84	60.5	60.5	0.90
46	80.7	80.9	0.98	88.2	80.9	1.00
47	84.7	80.9	1.00	107.8	80.9	0.96
48	84.3	80.9	1.00	143.7	80.9	0.96
49	80.9	80.9	1.00	89.8	80.9	1.00
50	82.3	80.9	1.00	89.8	80.9	0.98
51	40.2	80.9	0.76	40.8	40.8	1.01
52	38.8	80.9	0.74	39.8	39.8	1.03
53	37.8	80.9	0.70	37.9	37.9	1.00
					Min	0.70
					Max	1.12
					Mean Value	***0.94***
					Standard Deviation	***0.10***
					Coefficient of Variation	***0.11***

675